



32 anticipated to exceed 51 cm by 2100 under an unchecked emission growth scenario (Bamber and  
33 others, 2019). Between 2010 and 2017, Arctic glaciers (excluding the Greenland Ice Sheet (GrIS) and  
34 its peripheral glaciers) lost  $609 \pm 7$  Gt of ice, equating to a sea-level rise of  $0.240 \pm 0.007$  mm a<sup>-1</sup> (Tepes  
35 and others, 2021a). During this period (excluding the GrIS and peripheral glaciers), the largest mass  
36 losses in the Arctic occurred in the southern Canadian Arctic ( $-606 \pm 44$  kg m<sup>-2</sup> a<sup>-1</sup>) and in the Russian  
37 High Arctic, comprising the archipelagos of Franz Josef Land, Novaya Zemlya, and Severnaya Zemlya  
38 (Noël and others, 2018; Zemp and others, 2019; Tepes and others, 2021a). Within the Russian High  
39 Arctic, mass loss was dominated by Novaya Zemlya in the far west of the Russian High Arctic ( $-385 \pm$   
40  $18$  kg m<sup>-2</sup> a<sup>-1</sup>) (Tepes and others, 2021b).

41 Atmospheric warming is the primary driver of Arctic glacier loss, whereas oceanic warming  
42 has been largely restricted to Atlantic-influenced Greenland and the western Russian High Arctic  
43 (Straneo and Heimbach, 2013; Carr and others, 2017a; Sommer and others, 2022; Tepes and others,  
44 2021b). The inflow of warmer Atlantic waters into the Eurasian Basin is a key driver of glacier retreat  
45 in the Russian High Arctic and has resulted in reduced sea ice concentrations surrounding Novaya  
46 Zemlya, allowing for heat fluxes to rise through the water column, interacting with the atmosphere  
47 (Polyakov and others, 2017; Tepes and others, 2021b). By comparison, there are higher sea ice  
48 concentrations and a more pronounced ocean stratification towards Severnaya Zemlya, reducing  
49 such ocean-atmosphere heat transfer and resulting in much lower atmospheric temperatures (Tepes  
50 and others, 2021b). However, regions as far east as Severnaya Zemlya, which were previously thought  
51 to be less sensitive to ocean-climate warming, are now undergoing accelerated glacier mass loss,  
52 attributed to increasing oceanic temperatures. Notably, Severnaya Zemlya has undergone a 29%  
53 increase in specific glacier mass loss from 2003 to 2009 and 2010 to 2017 (Tepes and others, 2021b).

54 In recent years, Severnaya Zemlya's glaciers have not only undergone accelerated mass loss  
55 (Sommer and others, 2022), but also increasing glacier flow speeds, with some notable 'surging'  
56 activity linked to a switch in basal thermal regime (Strozzi and others, 2017). Most notable of these  
57 was the destabilisation of the western basin of the Vavilov Ice Cap, which transitioned from land to  
58 marine-terminating and advanced >8 km (Willis and others, 2018). In general, however, research on  
59 Severnaya Zemlya has been hindered by inaccessibility and poor data availability, hence both the very  
60 recent and long-term trends in glacial retreat/advance are largely unknown compared to elsewhere  
61 in the European High Arctic (e.g., Novaya Zemlya and Svalbard). The recent availability of new high-  
62 resolution imagery (e.g., Sentinel-2A and ArcticDEM) and gravimetry and altimetry data (e.g., GRACE  
63 and ICESat) has led to an increase in research on Severnaya Zemlya, which has focused on ice surface  
64 elevation changes and overall mass balance estimates (e.g., Sharov and Tyukavina, 2009; Ciraci and  
65 others, 2020; Tepes and others, 2021b). However, whilst mass balance estimates are known for the

66 last few decades, it is not known how changes in mass balance manifest as changes in glacier surface  
67 area, nor how different types of glaciers on Severnaya Zemlya (e.g., marine and land-terminating  
68 glaciers and surge-type glaciers) are responding to climatic drivers over longer time-scales. This can  
69 be understood by interpreting a record of glacier area change, but no long-term record currently  
70 exists.

71 A record of long-term glacier change may be complicated by the presence of surge-type  
72 glaciers on Severnaya Zemlya (Dowdeswell and Williams, 1997; Glazovsky and others, 2015; Sánchez-  
73 Gámez and others, 2019). Climate is thought to be a first-order control on surge-type glacier  
74 distribution and recent work suggests that glaciers in cold, dry environments, such as the eastern  
75 Russian High Arctic, are less likely to be surge-type (Sevestre and Benn, 2015; Benn and others, 2019).  
76 However, surging has often been documented in polythermal and predominantly cold-based glaciers,  
77 such as in the Canadian High Arctic (e.g., Copland and others, 2003; Van Wychen and others, 2016),  
78 which is comparable to the largely cold-based glaciers and ice caps on Severnaya Zemlya. The recent  
79 and well-documented destabilisation of the Vavilov Ice Cap (Willis and others, 2018; Zheng and others,  
80 2019) and the identification of two surge-diagnostic looped medial moraines on the Karpinsky Ice Cap  
81 (Dowdeswell and Williams, 1997) are significant in that they provide clear evidence of glacier surging  
82 on Severnaya Zemlya. However, the wider distribution/existence of surge-type glaciers on Severnaya  
83 Zemlya is largely unknown and is important for understanding the relationship between glacier  
84 surging and climate, a relationship that is perhaps subject to alteration on Severnaya Zemlya under  
85 future climatic change. Indeed, most observations of surging are from temperate and polythermal  
86 glaciers (e.g., Kamb and others 1985; Raymond, 1987; Fowler and others, 2001; Quincey and others,  
87 2011) and additional documentation of surging in mostly cold-based glaciers is beneficial for assessing  
88 whether their characteristics and geomorphological signature differ.

89 In this paper, we use imagery from 1965 to 2021 to assemble the first long-term record of  
90 glacier change on Severnaya Zemlya and explore spatial and temporal trends in relation to ocean-  
91 climate forcing. This includes the identification of surge-type glaciers on the archipelago by  
92 systematically investigating each glacier for glaciological and geomorphological features diagnostic of  
93 surging (following Grant and others, 2009). This record of glacier change can be used as a basis for  
94 understanding and ascertaining the impact of climatic changes on Severnaya Zemlya.

95

96

97

## 98 2. STUDY AREA & PREVIOUS WORK

### 99 2.1. Location and Glacial History

100 Severnaya Zemlya is situated north of the Taymyr Peninsula, with Franz Josef Land and Novaya Zemlya  
101 to the west and southwest, respectively (Fig. 1). The archipelago is located between the Kara and  
102 Laptev seas and is less influenced by warmer Atlantic waters than Novaya Zemlya to the west, with  
103 lower rates of precipitation than in the Barents-Kara Seas (Timokhov, 1994; Schauer, and others,  
104 2002). Glaciers further east in the Russian High Arctic are characterised by a colder thermal structure,  
105 with glaciers on Severnaya Zemlya likely to be mostly frozen to their bed (Dowdeswell and Williams,  
106 1997). Mean annual precipitation and temperature on Severnaya Zemlya as recorded at the Vavilov  
107 Station (Fig. 1) were 423 mm water equivalent and -16.5 °C, respectively, for the period 1974-1988  
108 (Bassford and others, 2006b). The study area encompasses all glaciers on Severnaya Zemlya, which  
109 covered a total area of 17,500 km<sup>2</sup> in the glacier inventory of the USSR compiled between 1940-1970  
110 (Grosval'd and Kotlyakov, 1969). A re-survey from imagery acquired between 2000 and 2010 for the  
111 Randolph Glacier Inventory (RGI) 6.0 has since estimated the glacierised area to be 16,700 km<sup>2</sup>  
112 (Moholdt and others, 2012a; Khromova and others, 2014).

113 The 1940-70 USSR inventory estimated mean glacier thickness and volume to be 200 m and  
114 3,500 km<sup>3</sup>, respectively (Grosval'd and Kotlyakov, 1969). Glacier coverage increases towards the north,  
115 with glaciers covering 99.7% on the northwesternmost island, Schmidt Island, and most glacier volume  
116 in the Academy of Sciences Ice Cap on Komsomolets Island (Fig. 1; Sharvov and Tyukavina, 2009). To  
117 the southeast of the Academy of Sciences Ice Cap, the highest elevation is the peak of the Karpinsky  
118 Ice Cap, which reaches an altitude of 963 m (Sharov and Tyukavina, 2009). Most of the larger glaciers  
119 drain towards the eastern coast, with 26 outlet glaciers terminating in the Laptev Sea (Sharov and  
120 Tyukavina, 2009). Where data exist, the eastern outlets display higher velocities (e.g., Academy of  
121 Sciences Ice Cap Basins C & D - avg. 543 m a<sup>-1</sup> (2016-17)) than the five to six slow-moving outlet glaciers  
122 flowing into the Kara Sea to the west (Academy of Sciences Ice Cap Basin A - 240 m a<sup>-1</sup>) (Sharov and  
123 Tyukavina, 2009; Sánchez Gámez and others, 2019).



124

125 **Fig. 1.** Location map of Severnaya Zemlya (Severnaya Zemlya) and its distribution of glaciers from the 2001 -  
 126 2010 Randolph Glacier Inventory (RGI Consortium, 2017). The locations of previously identified surge-type  
 127 glaciers are mapped as follows: (a, green) basins A & B of the Academy of Science Ice Cap where surge-like  
 128 elevation changes were identified by Sánchez-Gómez and others (2019); (b, red) the two looped medial moraines  
 129 identified by Dowdeswell and Williams (1997). (c, blue) The location of the observed surge of the Vavilov Ice Cap  
 130 documented by Glazovsky and others (2015).

131

132 The extent of the Late Pleistocene glaciation during Marine Isotope Stage 2 (including the last  
 133 glacial maximum (LGM)) is controversial on Severnaya Zemlya. The eastern margins of the former  
 134 Barents-Kara Ice Sheet are unknown but are generally assumed to have reached the Taymyr Peninsula

135 and not extended onto Severnaya Zemlya (Svendsen and others, 1999; 2004; Polyak and others, 2008;  
136 Hughes and others, 2016). The interpretation of lacustrine proxies on October Revolution Island  
137 suggests that it has not been covered by extensive glaciation since marine isotope stage 5d-4 (Early  
138 Middle Weichselian; Raab and others, 2003). A change to colder, drier conditions at ~22 ka following  
139 an interstadial period triggered ice cap growth, with the LGM in the Russian Arctic being reached  
140 around 20-15 ka BP (Hubberten, and others, 2004). However, the LGM on Severnaya Zemlya was likely  
141 constrained close to modern margins, with the Vavilov Ice Dome believed to be small or non-existent  
142 (Raab and others, 2003; Svendsen and others, 2004). No evidence of glacial deposits was found in a  
143 lake core from southern Bolshevik Island, supporting these assumptions (Cherezova and others, 2020).  
144 Additionally, local evidence for ice grounding on the East Siberian continental margin during the LGM  
145 suggests that the purported East Siberian ice sheets did not extend to Severnaya Zemlya (Niessen and  
146 others, 2013).

147 In the Russian High Arctic, the Pleistocene - Holocene transition was characterised by  
148 warming, punctuated with cooling correlated with the Younger Dryas. This was followed by an early  
149 Holocene warming peak at 10,000-9,700 yr BP, reaching the Boreal then Holocene thermal maxima at  
150 ~8500 and ~5500 yr BP, respectively (Andreev and Klimanov, 2000). On Franz Josef Land, glaciers  
151 remained behind present margins from ~9.4 - 4.4 kyr, advancing to reach present margins by 2 kyr  
152 (Lubinski and others, 1999). Prominent neogacial advances are recorded at ca. 1 kyr on Franz Josef  
153 Land and, on Novaya Zemlya, neogacial moraine sequences are situated within 4 km of present  
154 margins and dated to 1300 and 800 yr BP. This was followed by the Little Ice Age (LIA) advances and  
155 subsequent widespread retreat (Forman and others, 1999; Lubinski and others, 1999). No distinct  
156 signal of the Medieval Climate Anomaly or the LIA is readily detectable in the  $\delta^{18}\text{O}$  ice core record  
157 from the Academy of Sciences Ice Cap (Severnaya Zemlya), suggesting they may have not been  
158 pronounced in the Barents-Kara Sea region (Opel and others, 2013). A cold period at ~1800 followed  
159 by subsequent warming is interpreted to mark the termination of the LIA (Opel and others, 2013),  
160 although without establishing a chronology on moraine formation on Severnaya Zemlya this cannot  
161 be correlated with moraine stabilisation at surrounding localities.

162

## 163 **2.2. Recent Glacier Change**

164 No studies have assessed spatial and temporal changes in glacier extent on Severnaya Zemlya over  
165 the last few decades, with research primarily focusing on short-term changes in mass balance and ice  
166 flow dynamics (e.g., Bassford and others, 2006a; b; c; Tepes and others, 2021b). Several studies have  
167 used gravimetry and laser altimetry to assess recent volumetric changes of ice caps, concentrated on

168 the Academy of Sciences Ice Cap (e.g., Moholdt and others, 2012b; Sánchez-Gómez and others, 2019;  
169 2020; Tepes and others, 2021a; b). Most mass loss on Severnaya Zemlya is attributed to three outlets  
170 (ice streams *sensu lato*) on the Academy of Sciences Ice Cap which have thinned by  $> 1 \text{ m a}^{-1}$  and  
171 remained in a period of fast flow since 1995, notably Basins C & D, with basin A showing a three-fold  
172 increase in velocity and an increase in thickness at its terminus (Sharov and Tyukavina, 2009; Moholdt  
173 and others, 2012b; Nela and others, 2019; Sánchez-Gómez and others, 2019). On October Revolution  
174 Island, between 2012 and 2014, the main outlets of the Karpinsky Ice Cap thinned at a rate 3-4 times  
175 greater than the 30-year average following the collapse of the Matusevich Ice Shelf in 2012 (Moholdt  
176 and others, 2012b; Willis and others, 2015). In 2013, the western margin of the Vavilov Ice Cap  
177 destabilised and advanced 8 km, peaking at 25 m/day (Fig. 1c). This advance is thought to reflect the  
178 impact of changing basal boundary conditions on mostly cold-based ice caps, which may be related to  
179 climate warming (Willis and others, 2018; Zheng and others, 2019).

180

### 181 3. METHODS

#### 182 3.1. Image Acquisition and Processing

183 Satellite imagery was acquired for the years 1965/79, 1986, 1997, 2011, 2018 (DEM) and 2021 at  
184 intervals of  $\sim 10$  years to capture long-term changes (Supplementary Table S1). We use imagery from  
185 KH-7 and KH-9 'Hexagon', Landsat TM, Advanced Spaceborne Thermal Emission and Reflection  
186 Radiometer (ASTER), ArcticDEM, Sentinel-2A, and Landsat 8. Scenes were predominantly obtained  
187 from July to September when sea ice and snow cover are at a minimum and filtered for low cloud  
188 cover ( $< 10\%$ ), to ensure accurate delineation of glacier margins. All years have full glacier coverage  
189 except for 1965, which only covers October Revolution Island and Bolshevik Island and 1979, which  
190 only covers Komsomolets Island and Pioneer Island.

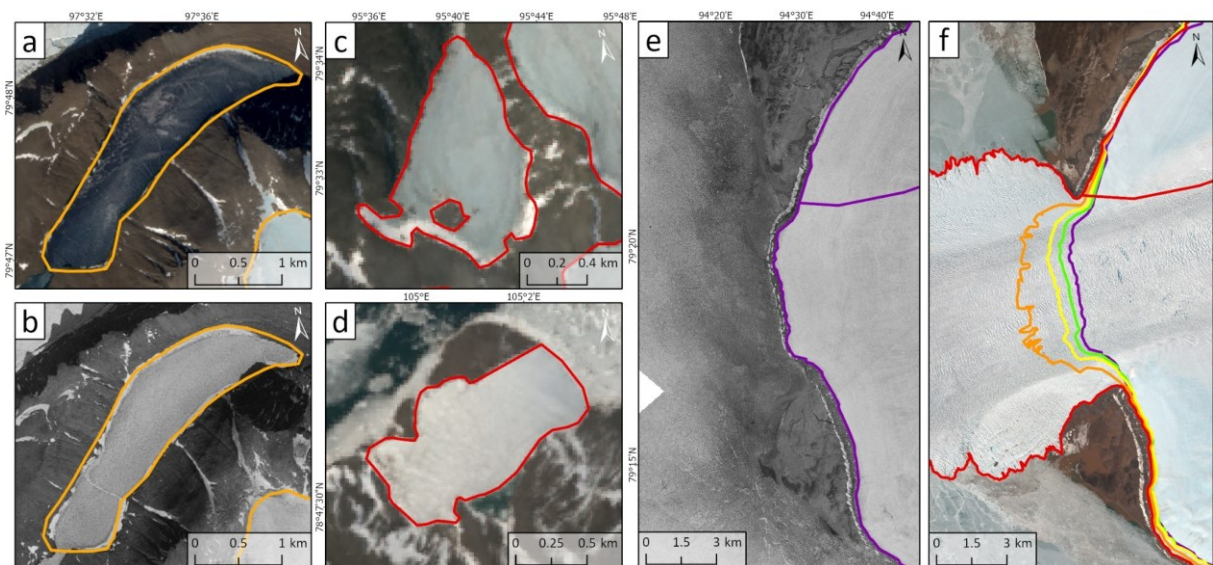
191 KH-7 and KH-9 imagery was manually georeferenced using a 2021 Sentinel-2A base layer and  
192 co-registered to a WGS 1984 Arctic Polar Stereographic projection. A total of 23 KH-7 and two KH-9  
193 single-image scenes were used to cover Severnaya Zemlya and were georeferenced using a spline  
194 transformation with  $\sim 30$  control points chosen per tile. Fixed points such as coastlines and bedrock  
195 features were used as control points, avoiding features subject to alteration (e.g., deltas and rivers).  
196 The transformations have a root mean square (RMS) value close to zero ( $\sim > 0.001$ ), providing a good  
197 assessment of the transformation accuracy, although minor errors in aligning control points may not  
198 be accounted for in the RMS value.

199

200 **3.2. Glacier Change Mapping and Uncertainties**

201 Using the RGI (Randolph Glacier Inventory) 6.0 data as a guide, glaciers were manually delineated  
202 using ESRI ArcGIS software, giving a total of 190 individual glacier units. Ice divides from the RGI data  
203 were used but that inventory could not be utilized in the analysis because the year of measurement  
204 was not the same for each glacier (2000 to 2010). Recently, a new inventory of Russian glaciers (2016-  
205 2019) by Khromova and others (2021) in Global Land Ice Measurements from Space (GLIMS) provided  
206 a more up-to-date record of glacier change on Severnaya Zemlya, however, this too uses different  
207 years of measurement for each glacier. The long-term record of satellite imagery in this study also  
208 allowed for the rectification of obvious misclassifications in the RGI inventory using some of the glacier  
209 identification criteria in Leigh and others (2019). This includes six new glaciers that have since  
210 detached from large ice caps or that may have been overlooked as snow patches in the RGI and one  
211 lake misclassified as a glacier in both the RGI and GLIMS (Fig. 2). Thereafter, each glacier was manually  
212 digitised using a Lambert Equal Area Projection for 1965, 1979, 1986, 1997, 2011 and 2021 (Fig. 2).  
213 Each glacier was given an ID from 1-190 for identification purposes (see supplementary spreadsheet  
214 1). Some linear snow patches may contain glacier ice, but do not meet the criteria for glacier  
215 identification (see Leigh and others, 2019) so are excluded from the mapped glaciated area for  
216 Bolshevik Island. Despite the panchromatic KH-7 and KH-9 imagery, the textural differences between  
217 glaciers, sea ice and land cover are clear and do not provide difficulties in delineating glacier area (Fig.  
218 2e; Leigh and others, 2019). Glacier area was calculated in km<sup>2</sup> for each year using ArcGIS Pro to  
219 establish rates of glacier surface area change. No classification of terminus type exists for Severnaya  
220 Zemlya, so each glacier unit was classified into one of three terminus types: marine-terminating, land-  
221 terminating, and lake-terminating.

222



223 **Fig. 2.** (a) RGI outlines (orange) overlaid over 2021 Sentinel-2A imagery of a lake misidentified as a glacier in  
224 the RGI. (b) RGI outlines overlaid on 1965 imagery - note the difference in surface texture between the lake and  
225 the glacier to the southeast and an absence of any features indicative of glacier ice (following Leigh and others,  
226 2019). (c) New glacier that has separated from a larger ice cap (glacier 187). (d) Small glacier not identified by  
227 the RGI (glacier 174). (e) Delineation of 1965 Vavilov extent (purple). (f) Glacier outlines for 1965, 1986 (green),  
228 997 (yellow) and 2011 (orange) superimposed on 2021 Sentinel-2A imagery.

229

230 Errors in manual glacier delineation were calculated following DeBeer and Sharp (2007), who  
231 assumed that line placement uncertainty is unlikely to be larger than the imagery resolution for debris-  
232 free glaciers on cloud-free imagery. They suggested that measurement error can be approximated by  
233 the polygon perimeter x the pixel resolution; for example, the area of glacier 1 = 120 km<sup>2</sup> and it has a  
234 perimeter of 66307 m and was mapped from 10 m ground pixel resolution imagery. Thus, the line  
235 placement/mapping uncertainty is  $120 \pm 0.66$  km<sup>2</sup>. Errors are calculated for each glacier unit at each  
236 date (see supplementary spreadsheet 1), with measurement errors for the total area detailed in Table  
237 2.

238

### 239 **3.3. Climate Data**

240 Daily air temperatures were obtained from two stations: Im. E. K. Fedorova (WMO code 20292)  
241 (77.7°N, 104.3°E, 12 m a.s.l., 1936-2021) at the north of the Taymyr Peninsula, south of Bolshevik  
242 Island; and Ostrov Golomjannyj (WMO code 20087) (79.6°N, 90.6°E, 8 m a.s.l., 1936-2021) on  
243 Golomjannyj Island 40-50 km west of October Revolution Island (see Fig. 1). Annual summer (1st June  
244 to 31st August) and winter (1st Dec - 28/29th February) means were computed for each station, with  
245 anomalies calculated from the long-term (1936 - 2021) mean. Data used for climate plots were  
246 accessed from the National Oceanic and Atmospheric Administration (NOAA)  
247 (<https://www.noaa.gov/>). Long-term (1981 to 2022) composite plots of surface skin temperature  
248 ( $SST_{skin}$ ), precipitation and air temperature (2 m) were produced from NOAA plotting tools, which use  
249 National Centres for Atmospheric Prediction (NCEP) re-analysis data. Surface skin temperature refers  
250 to the temperature of water at a depth of ~10 to 20 micrometres. Additionally, NCEP re-analysis data  
251 were used to compare recent 21<sup>st</sup>-century climatic changes (2000 to 2022) against the climate normal  
252 time period (1991 to 2020).

253

254

255

256 **3.4. Identification of surge-type glaciers**

257 Each of the 190 glaciers on Severnaya Zemlya was examined for the presence or absence of features  
258 that may be diagnostic of surging (Table 1). These criteria for identifying surge-type glaciers have been  
259 adapted from Grant and others (2009) and Copland and others (2003) and modified to reflect that we  
260 did not observe any smaller-scale subglacially-derived components in our imagery (e.g., crevasse-  
261 squeeze ridges). Each criterion was weighted to reflect whether it is primarily diagnostic of surging  
262 (e.g., looped medial moraines) or may only be diagnostic of surging in conjunction with other criteria  
263 (e.g., heavy surface crevassing) (Table 1). The highest weighting of 5 was assigned to looped medial  
264 moraines and localised abnormal advances as they are robust indicators of surging (Meier and Post  
265 1969; Lawson, 1996; Evans and Rea, 1999; 2003; Hewitt, 2007; Paul, 2015). Due to potential  
266 equifinality associated with thrust block/glacitectonic composite moraines (4) and crevassing up  
267 glacier (3), they are not weighted high enough to individually result in a surge-type classification  
268 (Fitzsimons, 1996; 1997, 2003; Evans and Rea, 1999; 2003; Evans, 2009; Benn and Evans 2010).  
269 However, they are weighted more heavily than supraglacial ponding (1) and shear margins (1).  
270 Following weighting, each glacier is classified as either category 1 - confirmed surge-type (>10, active  
271 phase observed and 3 surge-indicative criteria present), category 2 - likely to have surged (>7, indirect  
272 evidence), category 3 - possible surge-type (4-6, indirect evidence) or non-surge-type (0-3). Glaciers  
273 are only classified as confirmed surge-type if a localised anomalous advance has been observed during  
274 the study period (which is assumed to be the active phase) and if three other surge-indicative criteria  
275 are present. Where localised anomalous advances occur but are only short-lived and minor, we do not  
276 consider these to be an active phase and instead restrict their classification to likely to have surged.  
277 We acknowledge that our method is biased towards the surge classification of land-terminating  
278 glaciers because of the additional criteria that may be present within their exposed forelands (as  
279 opposed to submarine geomorphology proximal to marine-terminating glaciers but we are not aware  
280 of any bathymetric datasets available around Severnaya Zemlya.

281

Criteria	Description	Weighting
<b>Glaciological</b>		
Looped moraines	Produced when medial moraines are deformed due to the combination of fast- and slow-flowing ice within adjacent glaciers	5
Localised abnormal advance	Indicative of the active phase of the surge cycle	5
Highly digitate terminus	Terminus is splayed into lobes by longitudinal crevasses	3
Heavy surface crevassing up-glacier	Indicative of the active phase of the surge cycle and develop due to increased longitudinal stresses	3
Deformed ice structures	Form in a similar manner to looped moraines	1
Shear margins	Develop at the boundary between fast- and slow-flowing ice	1
Heavy surface crevassing at the terminus	Formed during the surge phase	1
Surface Potholes	Typically appear during the quiescent phase; they form in crevasses formed during the surge phase or in depressions between transverse ridges	1
<b>Geomorphological</b>		
Thrust-block/push moraines	Form as a result of marginal thrusting due to ice advance into proglacial sediments and can form in belts of arcuate thrust ridges. In areas where sediment is limited, low-amplitude push moraines develop	4
Overridden thrust-block moraines	Formed thrust blocks are overridden by ice and form ice-moulded 'cupola' hills	1
Hummocky moraine	Produced in belts at the margin of glaciers and consist of chaotic landscape with kame and kettle topography, which evolves from the thrusting, squeezing, and bulldozing of sediments and meltout of buried glacier ice (However, other origins are possible)	1

## 284 4. RESULTS

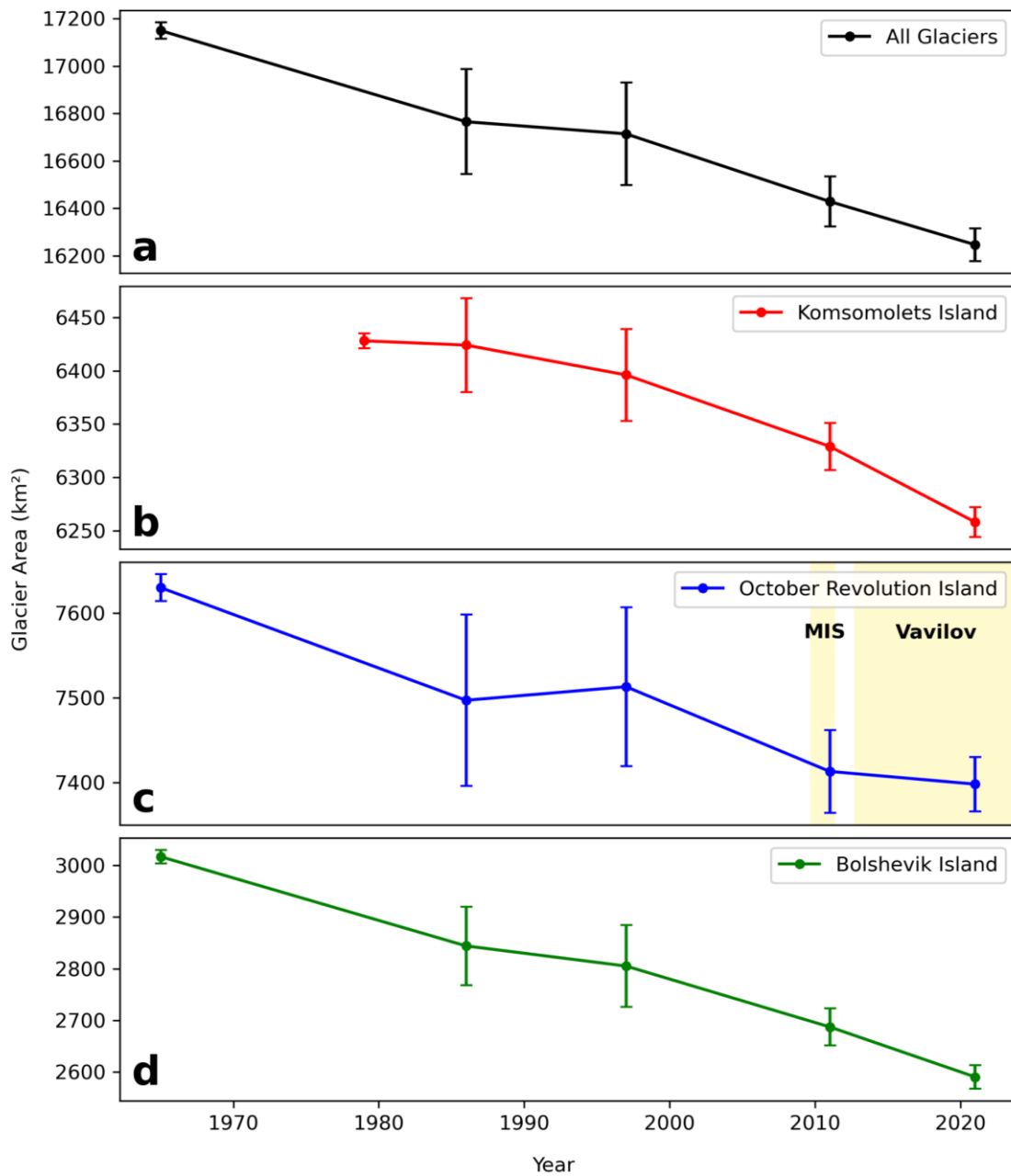
### 285 4.1. Glacier Change

286 Between 1965 ( $17,053 \pm 38 \text{ km}^2$ ) and 2021 ( $16,275 \pm 69 \text{ km}^2$ ), glaciers on Severnaya Zemlya lost a  
 287 combined area of  $778 \text{ km}^2$  (5% area decrease) at an average rate of  $13.9 \text{ km}^2 \text{ a}^{-1}$  (Table 2; Fig. 3). By  
 288 region, Bolshevik Island accounts for 55% of glacier area loss ( $-426 \text{ km}^2$ ), October Revolution Island for  
 289 30% ( $-230 \text{ km}^2$ ), and Komsomolet, Pioneer and Schmidt islands for 16% ( $-122 \text{ km}^2$ ). From 1965 to 2021,  
 290 95.7% of glaciers showed a decline in surface area and 8 glaciers increased in overall area, with 10  
 291 separate advances ( $> 0.5 \text{ km}^2$  and exceeding error margins) recorded between these dates (Table 2;  
 292 supplementary spreadsheet 1). The mean glacier areal shrinkage between 1965 and 2021 was -17%,  
 293 however, one very small glacier (glacier 178) disappeared during this time period, with others (e.g.,  
 294 glacier 87, -93%) also undergoing large shrinkages.

295            In terms of temporal changes, glaciers and ice caps shrank at a rate of  $-13.3 \text{ km}^2 \text{ a}^{-1}$  between  
296 1965/79 and 1986, which decreased to  $-5.5 \text{ km}^2 \text{ a}^{-1}$  between 1986 and 1997. However, due to the  
297 larger error margins for 1986 and 1997, there is low confidence in a significant deceleration in retreat  
298 rate (Table 2; Fig. 3). A notable acceleration in retreat is recorded between 1997 and 2011 ( $-20.3 \text{ km}^2$   
299  $\text{a}^{-1}$ ), which continues through to 2011 - 2021 ( $-15.4 \text{ km}^2 \text{ a}^{-1}$ ).

300 **Table 2.** Summary statistics of glacier surface area change on Severnaya Zemlya. Uncertainties are provided for the overall and regional total areas (for individual glaciers see  
 301 supplementary spreadsheet 1).

	1965(*79)	1986	1997		2011		2021		1965 - 2021		
	Area (km <sup>2</sup> )	Area (km <sup>2</sup> )	Change (km <sup>2</sup> a <sup>-1</sup> )	Area (km <sup>2</sup> )	Change (km <sup>2</sup> a <sup>-1</sup> )	Area (km <sup>2</sup> )	Change (km <sup>2</sup> a <sup>-1</sup> )	Area (km <sup>2</sup> )	Change (km <sup>2</sup> a <sup>-1</sup> )	Change (km <sup>2</sup> )	Change (km <sup>2</sup> a <sup>-1</sup> )
All Glaciers	17053.4±38	16774.2±221	-13.3	16713.9±216	-5.48	16429.2±22	-20.34	16275.4±69	-15.4	-778.1	-13.9
Mean	90.1	90.2	-0.1	89.9	0.0	90.6	-0.1	85.7	-0.1	-2.2	-0.1
Median	21.8	21.8	0.0	21.6	0.0	22.4	-0.1	19.7	-0.1	-1.8	0.0
SD	173.4	174.1	0.3	174.3	0.2	175.0	0.2	171.6	0.1	16.1	0.3
Min	0.4	0.4	2.9	0.2	1.8	0.5	0.1	0	0.0	141.5	2.5
Max	1243.7	1246.2	-2.0	1246.1	-0.7	1243.7	-1.7	1243.1	-1	-42.8	-1.8
Komsomolets, Pioneer & Schmidt*	6407.8±7	6422.3±44	2.1	6395.8±44	-2.4	6328.7±22	-4.8	6285.5±30	-4.3	-122.3	-2.2
Mean	305.1	305.8	0.1	304.6	-0.1	301.4	-0.2	299.3	-0.2	-5.8	-0.1
Median	157.7	157.7	0.0	157.2	0.0	155.7	-0.1	154.8	-0.1	-0.7	0.0
SD	363.2	366.3	0.8	365.8	0.3	364.6	0.4	363.6	0.5	11.3	0.3
Min	1.3	1.4	2.9	1.9	0.4	0.7	0.2	0.5	0.4	3.9	0.1
Max	1243.7	1246.2	-1.1	1246.1	-0.7	1243.7	-1.1	1243.1	-1.6	-39.9	-3.0
October Revolution (-Vavilov)	7628.8±17	7507.6±101	-5.8	7513.2±98	0.5	7413.4±49	-7.1	7398.7±32	-1.5	-230.3	-4.1
Mean	117.4	115.5	-0.1	116.0	0.0	112.3	-0.1	112.1	0.0	-3.6	0.0
Median	58.2	55.6	0.0	55.3	0.0	54.4	0.0	53.8	0.0	-2.1	0.0
SD	144.6	142.6	0.3	144.0	0.3	142.5	0.3	143.4	1.8	23.3	0.4
Min	1.3	1.5	0.4	1.5	1.8	1.1	0.8	1.1	12.7	141.5	2.5
Max	594.1	594.8	-2.0	594.0	-0.4	593.3	-1.7	591.8	-5.4	-99.8	-1.8
Bolshevik	3016.6±13	2844.3±76	-8.2	2805.0±74	-3.6	2687.0±36	-8.4	2591.2±23	-9.6	-425.5	-7.6
Mean	30.8	28.4	-0.1	28.0	0.0	26.6	-0.1	25.2	-0.1	-4.5	-0.1
Median	11.3	9.8	0.0	9.6	0.0	8.2	0.0	7.4	-0.1	-2.0	0.0
SD	49.9	47.8	0.1	47.5	0.1	46.0	0.1	45.0	0.0	7.5	0.1
Min	0.5	0.4	0.0	0.2	0.0	0.2	0.0	0	0.0	1.2	0.0
Max	335.8	323.2	-0.8	320.0	0.0	306.5	-1.0	296.5	-1	-44.8	-0.8



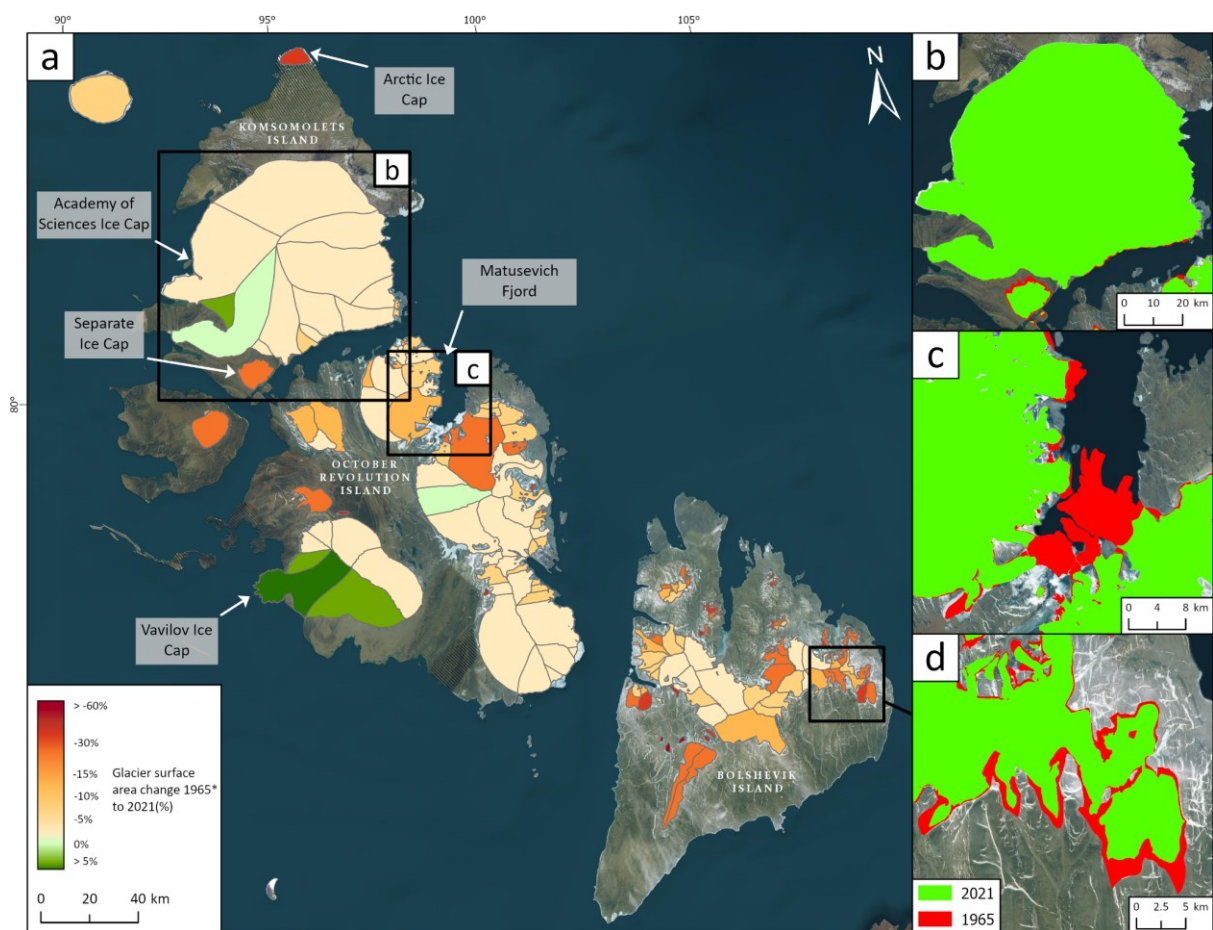
302

303 **Fig. 3.** Glacier change on Severnaya Zemlya by region. Errors bars reflect the minimum and maximum possible  
 304 extents of glacier area at each date. (a) Overall glacier change - note that data from Komsomolets Island in 1979  
 305 is included in the 1965 data point. (b) Glacier change on Komsomolets Island from 1979 to 2021. (c) Glacier  
 306 change on October Revolution Island from 1965 to 2021 - note the 2010 collapse of the Matushevich Ice Shelf and  
 307 the advance of the Vavilov Ice Cap post-2013 (in yellow). (d) Glacier change on Bolshevik Island from 1965 to  
 308 2021.

309

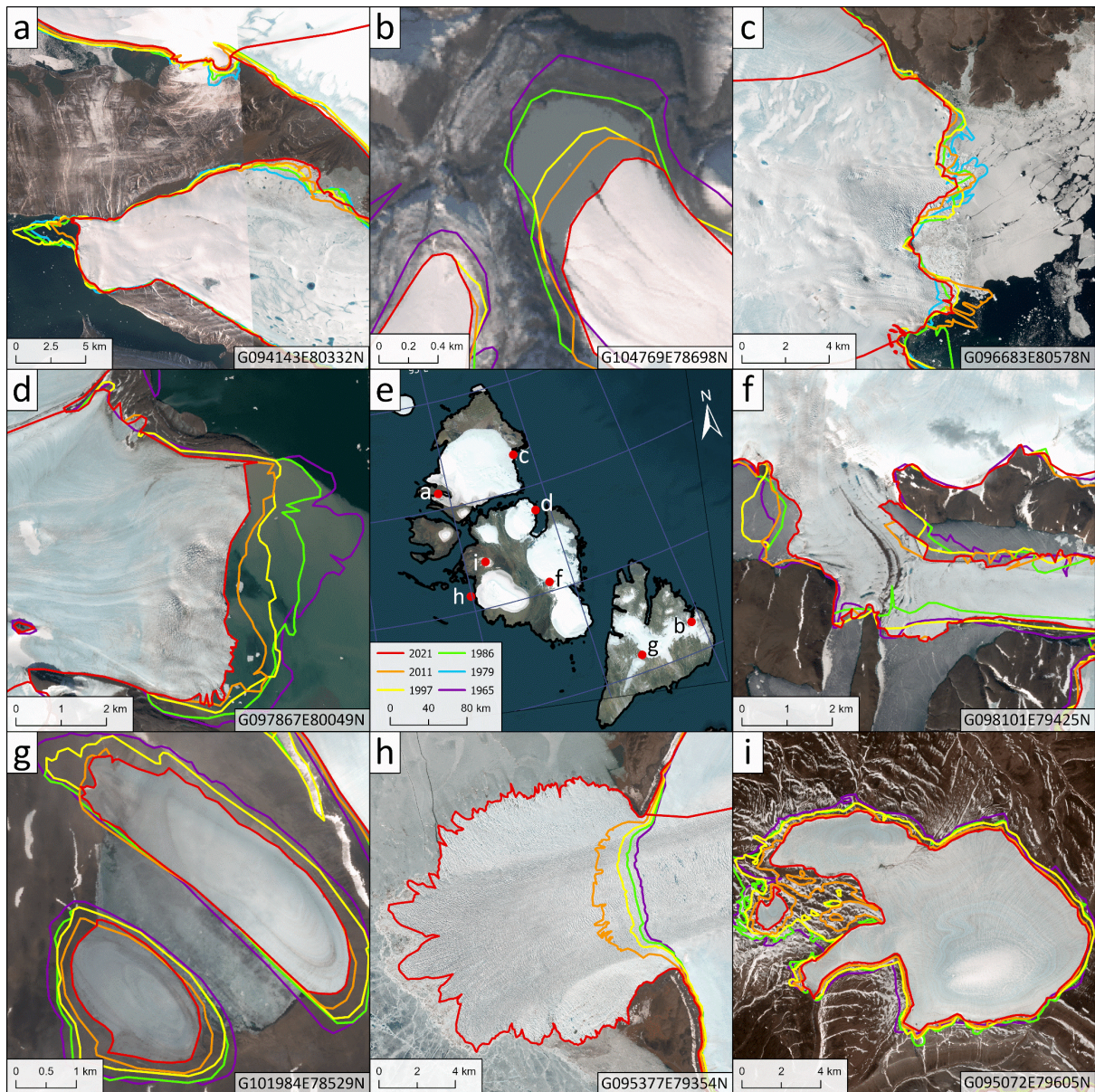
310 Komsomolets Island experienced the smallest amount of glacier retreat ( $-2.2 \text{ km}^2 \text{ a}^{-1}$ , 1979-  
 311 2021 = 1.9% area decrease), compared to southernmost Bolshevik Island ( $-7.6 \text{ km}^2 \text{ a}^{-1}$ , 1965-2021 = -  
 312 14.1% area decrease; Table 2; Fig. 3). Nonetheless, glaciers and ice caps on Komsomolets Island

313 underwent a progressive acceleration in retreat rates between each date, with a small increase in area  
 314 between 1979 and 1986 ( $2.1 \text{ km}^2 \text{ a}^{-1}$ ), followed by an acceleration in retreat rate between 1986 and  
 315 1997 ( $-2.4 \text{ km}^2 \text{ a}^{-1}$ ). Annual retreat rates doubled between the periods 1986-1997 and 1997-2011 ( $-4.8$   
 316  $\text{km}^2 \text{ a}^{-1}$ ) and decelerated slightly to  $-4.3 \text{ km}^2 \text{ a}^{-1}$  between 2011-2021, which is lower than the rate of  
 317 change on Bolshevik Island between 1965/79 and 1986 ( $-8.2 \text{ km}^2 \text{ a}^{-1}$ ). The largest rates of retreat (in  
 318 percentage terms) have preferentially occurred on the smaller Arctic Ice Cap (glacier 17) and Separate  
 319 Ice Cap (glacier 147), with minimal retreat of the Academy of Sciences Ice Cap (Fig. 4). Between  
 320 1965/79 and 2021, five separate advances (that exceed error margins) are recorded for the Academy of  
 321 Sciences Ice Cap, although only Basin A (Fig. 5a) and Glacier 154 showed an overall net increase in  
 322 area from 1965 - 2021.



323  
 324 **Fig. 4.** (a) Overall glacier surface area changes between 1965 and 2021 (%). Negative (red) and positive (green)  
 325 changes are scaled to reflect the amount of glacier change (b) Changes in glacier ice margins from 1965 (red) to  
 326 2021 (green) on the Academy of Sciences Ice Cap (top), note that ice margins have remained relatively stable. (c)  
 327 Changes in ice margins surrounding Matushevich Fjord and the breakup of the former Matushevich Ice shelf. (d)  
 328 Changes in ice margins on south-eastern Bolshevik Island.

329



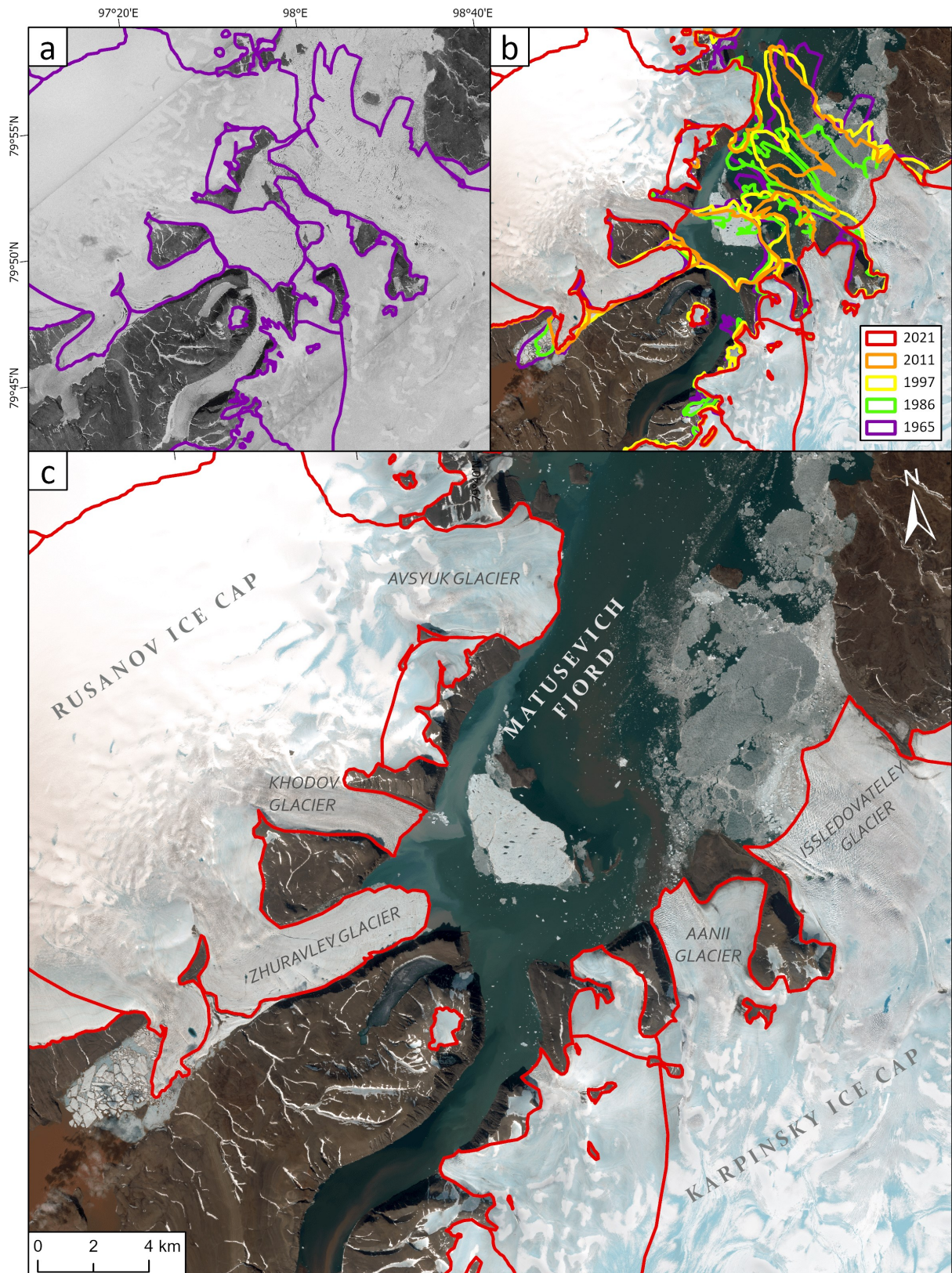
330

331 **Fig. 5.** Glacier change outlines at dates from 1965 - 2021 overlaid on 2021 Sentinel-2A imagery, including RGI  
 332 IDs. (a) Basin A of the Academy of Sciences Ice Cap. (b) Glacier 41 - retreated from controlled moraines damming  
 333 a proglacial lake. (c) Basin D of the Academy of Sciences Ice Cap. (d) Glacier 1 - marine-terminating on the north-  
 334 eastern margin of the Rusanov Ice Cap. (e) Location of glaciers shown within Severnaya Zemlya. (f) Glacier 105 -  
 335 observed to surge twice. (g) Glaciers 160 and 176 - lacustrine terminating glaciers on Bolshevik Island (h) surge  
 336 of the western Vavilov basin. (i) The separation of the Dezhnev Ice Cap.

337

338           Glaciers on October Revolution Island have undergone the second-highest rate of area loss on  
 339 Severnaya Zemlya, with a  $-4.1 \text{ km}^2 \text{ a}^{-1}$  surface area loss ( $-3.0\%$  area decrease) between 1965 and 2021  
 340 (Table 2). Net retreat between 1965 and 1986 ( $-5.8 \text{ km}^2 \text{ a}^{-1}$ ) was interrupted by an increase in overall  
 341 area between 1986 and 1997 ( $0.5 \text{ km}^2 \text{ a}^{-1}$ ), attributed to an advance from a western basin of the  
 342 Vavilov Ice Cap (41.18% increase in  $\text{km}^2$ ), which by 2021 had advanced 13.5 km from its 1965 position  
 343 (Fig 5H). Despite the continued advance of the Vavilov Ice Cap, the glaciated area of October

344 Revolution Island declined between 1997 and 2011 ( $-7.1 \text{ km}^2 \text{ a}^{-1}$ ), with the tributary glaciers feeding  
345 the former Matusevich Ice Shelf experiencing rapid retreat post-2012 (Fig. 6). Between 2011 and 2021,  
346 glaciers on October Revolution Island showed a reduction in retreat rate ( $-1.5 \text{ km}^2 \text{ a}^{-1}$ ). However, this  
347 overall rate of change is skewed due to a large gain in area from the advance of the Vavilov Ice Cap  
348 (Fig. 5h).



349

350 **Fig. 6.** Glacier area change in Matushevich Fjord. (a) The extent of the former Matushevich Ice shelf in 1965 KH-7  
 351 imagery. (b) Glacier change outlines from 1965 - 2021, note the advance of the Issledovateley glacier between  
 352 1986 and 2011. (c) The state of Matushevich Fjord in 2021, including glacier names.

353

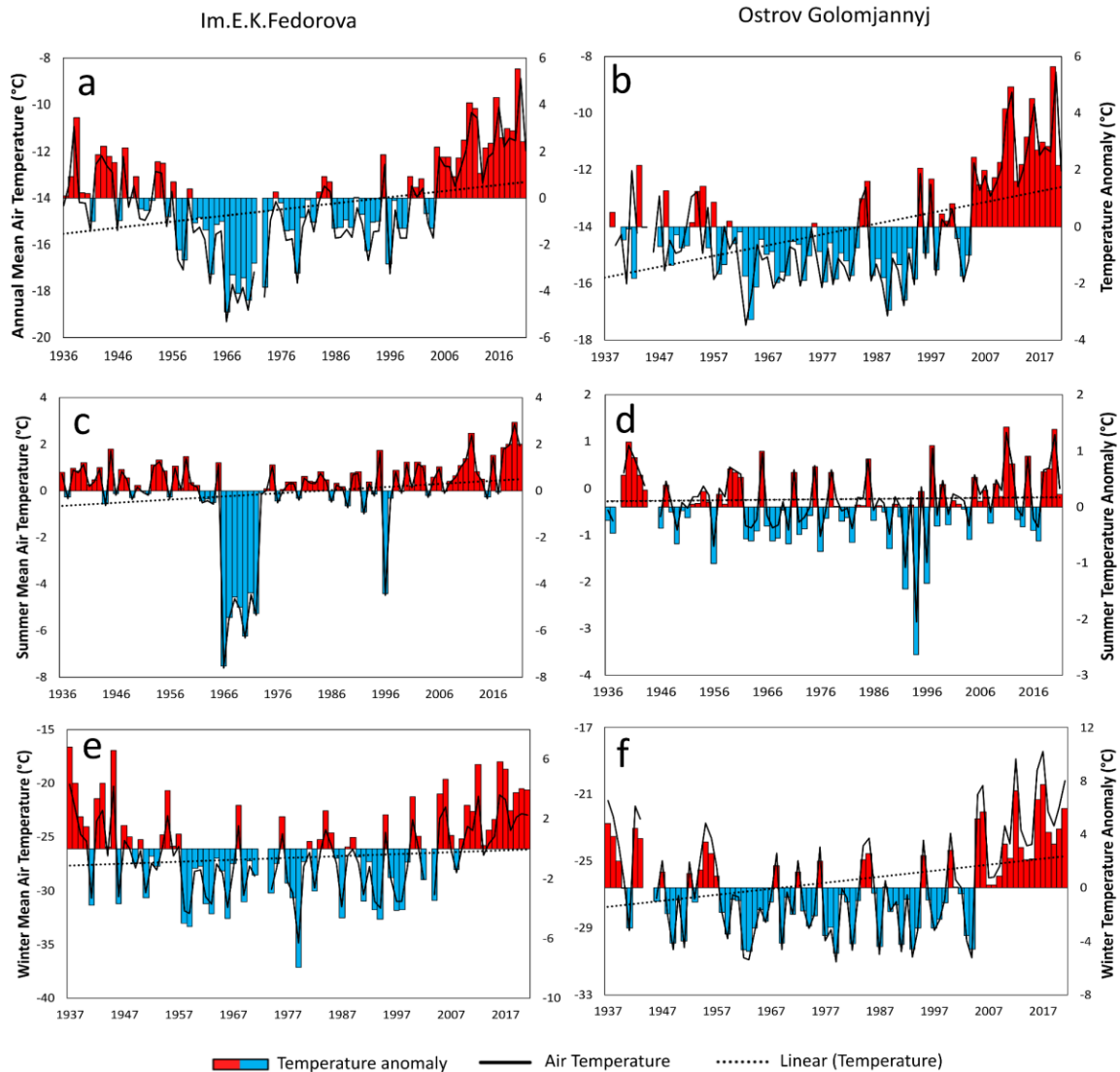
354 The southernmost island, Bolshevik Island, has shown the greatest reduction in glacier area of  
355  $-7.6 \text{ km}^2 \text{ a}^{-1}$  (-14.1% decrease,  $-426 \text{ km}^2$ ) from 1965 to 2021, with no advances recorded (Table 2).  
356 Between 1965 and 1986, glacier surface area declined at a rate of  $-8.2 \text{ km}^2 \text{ a}^{-1}$ , preferentially affecting  
357 small ice caps in the southwest of the island (Fig. 4). Glacier retreat rates declined to  $-3.6 \text{ km}^2 \text{ a}^{-1}$   
358 between 1986 and 1997, although the error margins are large due to the coarse imagery, so a  
359 significant deceleration in the retreat rate is uncertain. Post-1997, the rate of glacier retreat increased  
360 at each date, with the greatest increase in retreat rates occurring between 1986 and 1997 ( $-3.6 \text{ km}^2$   
361  $\text{a}^{-1}$ ) and 1997 and 2011 ( $-8.4 \text{ km}^2 \text{ a}^{-1}$ ). The fastest rate of retreat occurred between 2011 and 2021 ( $-$   
362  $9.6 \text{ km}^2 \text{ a}^{-1}$ ), which exceeded both Komsomolets ( $-4.3 \text{ km}^2 \text{ a}^{-1}$ ) and October Revolution islands ( $-1.5$   
363  $\text{km}^2 \text{ a}^{-1}$ ) during the same period.

364 The overall spatiotemporal trends in surface area change show a north-to-south gradient of  
365 increased retreat, concentrated on Bolshevik Island, where most glaciers are land-terminating (Fig. 4).  
366 Observations show a recent (post-1997) acceleration in retreat rates on northern Severnaya Zemlya,  
367 albeit not strongly on October Revolution Island, whereas glaciers on Bolshevik Island have notably  
368 retreated across the entire observational period (1965 to 2021) (Fig. 3).

369

#### 370 **4.2. Climate Change**

371 Continentally influenced Im. E. K. Fedorova ( $-14.4^\circ\text{C}$ , 1936-2021) and marine-influenced Ostrov  
372 Golomjannyj ( $-14.2^\circ\text{C}$ , 1937-2021) are characterised by similar annual air temperatures, despite Im. E.  
373 K. Fedorova being  $2^\circ$  further south (Fig. 1; Fig. 7a-b). A stronger trend in mean annual warming  
374 temperature is recorded at Ostrov Golomjannyj, which has warmed by  $3^\circ\text{C}$  ( $R^2 = 0.24$ ),  $1^\circ\text{C}$  more than  
375 at Im. E. K. Fedorova ( $R^2 = 0.10$ ), with both trends being statistically significant ( $p < 0.05$ ) (Fig. 7a-b). Im.  
376 E. K. Fedorova is characterised by warmer summers (average  $-0.08^\circ\text{C}$ , 1936-2021) and post-2000 has  
377 recorded a progressive increase in positive temperature anomalies (Fig. 7c). Ostrov Golomjannyj is  
378 characterised by slightly colder summers ( $-0.2^\circ\text{C}$ , 1936-2021) and shows no discernible trend of  
379 summer warming (Fig. 7d). Ostrov Golomjannyj ( $-26.2^\circ\text{C}$ , 1937-2021) has a similar winter temperature  
380 to Im. E. K. Fedorova ( $-26.9^\circ\text{C}$ ) despite being two degrees further north, and whilst both stations have  
381 seen an increase in positive temperature anomalies post-2005, only Ostrov Golomjannyj shows a  
382 statistically significant ( $p < 0.05$ ) linear trend in winter warming ( $R^2 = 0.08$ ) (Fig. 7e-f). Long-term trends  
383 from both stations show that the 1930s/40s were generally warmer than the long-term annual  
384 average (Im. E. K. Fedorova;  $-14.4^\circ\text{C}$ , Ostrov Golomjannyj;  $-14.1^\circ\text{C}$ ), followed by cooling between the  
385 1950s and 1990s, which was more pronounced at Im. E. K. Fedorova (Fig. 7a-f). Post-2000, both  
386 stations show rapid warming and consistent positive temperature anomalies (Fig. 7a-f).



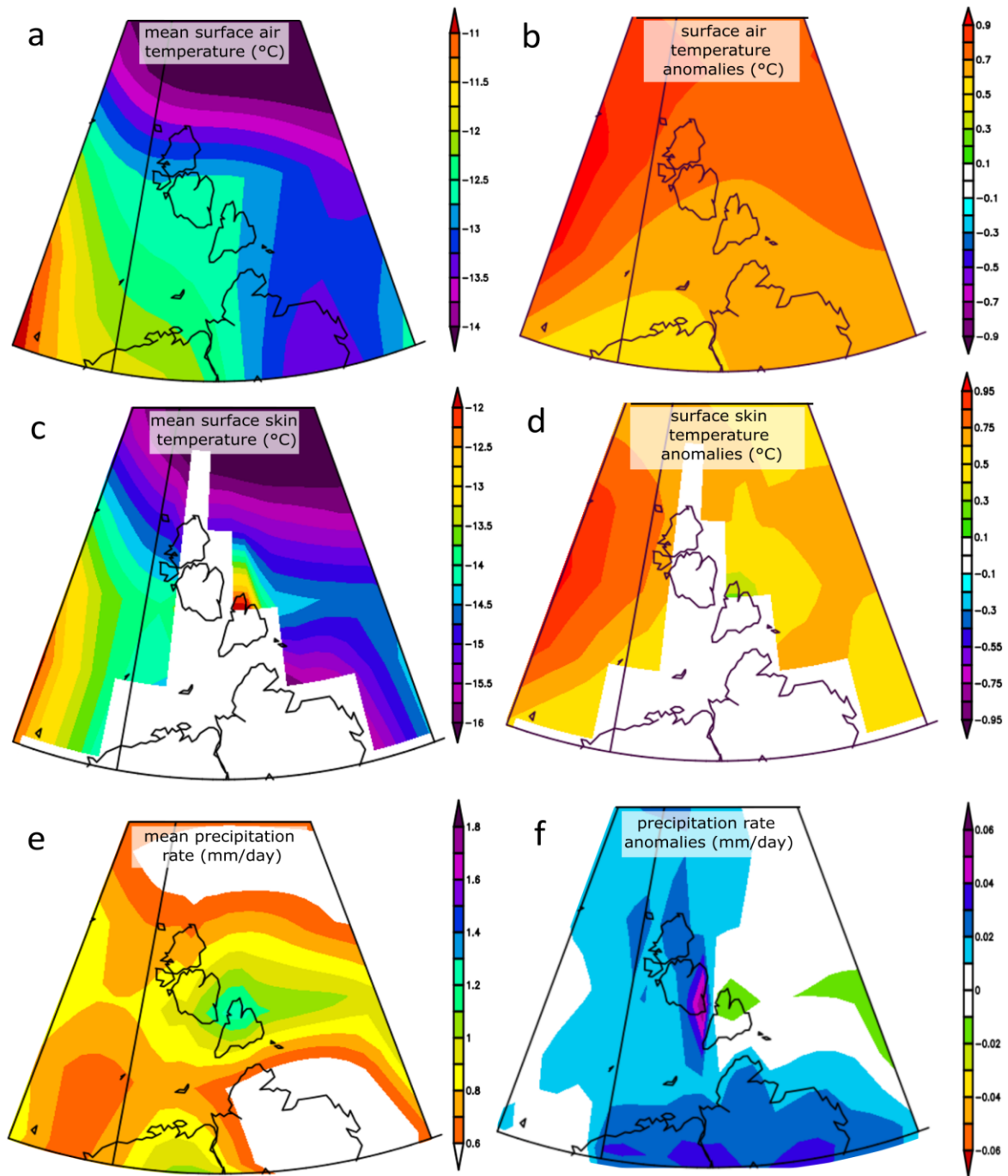
387

388 **Fig. 7.** Seasonal and annual average air temperatures at Im. E. K. Fedorova (left) and Ostrov Golomjannyj (right).  
 389 The location of each weather station is shown in figure 1. Negative anomalies (blue) and positive anomalies (red)  
 390 are shown by the bar chart, along with linear trend lines in surface air temperatures which are plotted against a  
 391 1936/7 to 2021 mean. Temperature is plotted on the primary axis (left), with anomalies on the secondary axis  
 392 (right). (a) Annual average air temperature at Im. E. K. Fedorova. (b) Annual average air temperature at Ostrov  
 393 Golomjannyj. (c) Summer average air temperature at Im. E. K. Fedorova. (d) Summer average air temperature at  
 394 Ostrov Golomjannyj. (e) Winter average air temperature at Im. E. K. Fedorova. (f) Winter average air temperature  
 395 at Ostrov Golomjannyj.

396

397 Long-term (1981-2022) spatial trends in surface air temperature show that the warmest  
 398 temperatures occurred on southern Severnaya Zemlya (western Bolshevik and October Revolution  
 399 Island) (Fig. 8a). Temperatures decrease northwards towards Komsomolets Island and to the east of  
 400 Bolshevik Island on the Laptev Sea coast (Fig. 8a). Since the 21<sup>st</sup> century, mean annual surface air  
 401 temperature has increased across the entirety of Severnaya Zemlya, with the strongest warming

402 concentrated around the northern cape, and the weakest trends of warming occurring on Bolshevik  
403 Island (Fig. 8b). Spatial trends in mean annual  $SST_{skin}$  mostly correspond with mean surface air  
404 temperature, with colder temperatures to the north and warmer temperatures on the Kara Sea coast  
405 (Fig. 8a; Fig. 8c). Note that the NCEP reanalysis dataset incorporates some classified meteorological  
406 stations (Kalnay and others, 1996), one of which is at the centre of the modelled isopleth bullseye  
407 effect of abnormally warm SSTs off northern Bolshevik Island. Thus, we deem it a probable cause of  
408 this effect, although cannot verify with any certainty. Positive  $SST_{skin}$  anomalies are highest in the Arctic  
409 and Kara Seas, with evidence of warming but to a lesser extent in the Laptev Sea (Fig. 8d). Negative  
410  $SST_{skin}$  anomalies are confined to the northern coast of Bolshevik Island and eastern October  
411 Revolution Island (Fig. 8d). The highest rates of precipitation have been historically concentrated  
412 around northern Bolshevik Island and southern October Revolution Island (Fig. 8e). Since 2000, mean  
413 annual precipitation rates have increased compared to the climate normal time period (1991 to 2020)  
414 on October Revolution and Komsomolets Islands, whereas they have undergone a slight decline  
415 around the precipitation high on Bolshevik Island (Fig. 8f).



416

417 **Fig. 8.** Long-term (1981-2022) mean annual climatologies (left) plotted using NOAA NCEP reanalysis  
 418 monthly/seasonal climate composite tools (available at: <https://psl.noaa.gov/>) (Kalnay and others, 1996).  
 419 Anomaly plots that show recent 21<sup>st</sup> century (2000 to 2022) trends plotted against the new climate normal time  
 420 period (1991 to 2020) (right). (a) Mean surface (2 m) air temperature (°C). (b) (2 m) air temperature anomalies  
 421 (°C). (c) Mean surface skin temperature (°C). (d) Surface skin temperature anomalies (°C). (e) Mean annual  
 422 precipitation (mm/day). (f) Mean annual precipitation anomalies (mm/day).

423

424

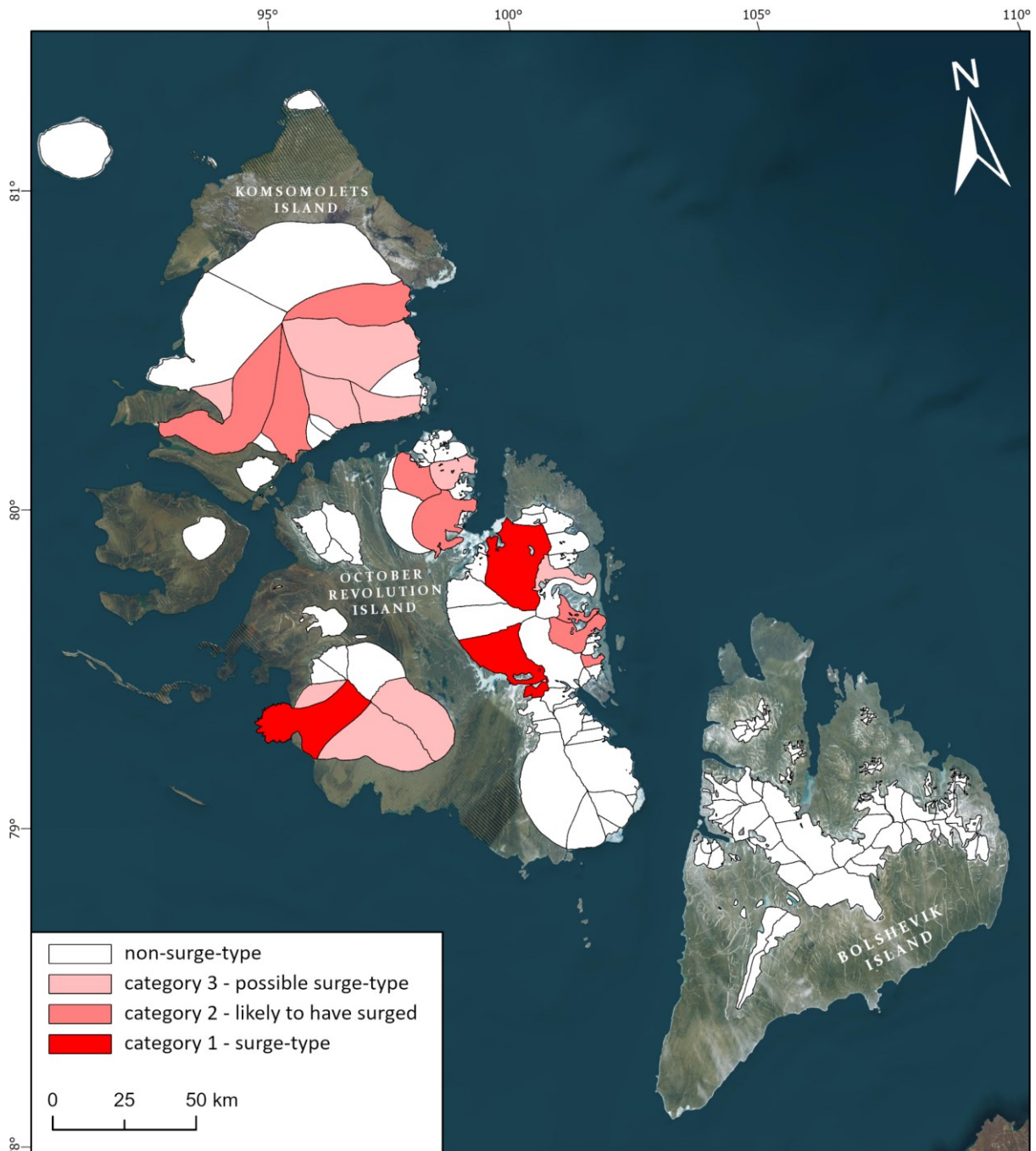
425 **4.3. Identification of surge-type glaciers**

426 The 190 glaciers on Severnaya Zemlya were systematically investigated for evidence regarded as  
427 diagnostic of active and former surging. Using the criteria in Table 1, it is suggested that three glaciers  
428 are of confirmed surge-type (category 1) (1.6%), eight are likely to have surged (category 2) (4.2%),  
429 and nine are possible surge-type (category 3) (4.7%) (Table 3; Fig. 9). Potential surge-type glaciers tend  
430 to be larger than non-surge-type glaciers, with those classified as confirmed surge-type representing  
431 8% of the 2021 glacier surface area of Severnaya Zemlya, likely to have surged representing 13%, and  
432 possible representing 15%. Where surging is identified, the most commonly identified surge-  
433 diagnostic features include surface potholes, a localised abnormal ice-front advance and heavy surface  
434 crevassing (Table 3).

435 **Table 3.** The presence of surge-type glaciers on Severnaya Zemlya. Lettering indicates the presence of a feature at an individual date: a. 1965, b. 1979, c. 1986, d. 1999,  
 436 e.2011, f.2021. A weighted total of 0-3 = non-surge, 4-6 = category 3 - possible surge-type, >7 = category 2 - likely to have surged, with glaciers classified as category 1 -  
 437 confirmed surge-type if they score >10, an advance is observed (active phase), and 3 or more surge-indicative features are present. See Table 1 for the weighting of each  
 438 criterion.

439

Glacier	Terminus	2021 Area (km <sup>2</sup> )	RGI ID	Looped/deformed medial moraines	Deformed ice structures	Shear margins	Surface crevassing up-glacier	Heavy surface crevassing at the terminus	Localised abnormal advance	Highly digitate terminus	Surface potholes	Thrust-block/push moraines	Total (weighted)
105	lacustrine	350.7	G098101E79425N	a	cdef		def	acd	c-e		acdef		16
128	marine	493.6	G098527E79706N				f	acdef	c-d	acde	acdef		13
76	marine	485.1	G095377E79354N			f	f	ef	e-f		cd		11
138	land	56.9	G099222E79553N	acdef						acdef		acdef	12
161	marine	145.6	G099370E79446N	acdef				acdef			acdef	acdef	11
93	marine	293.7	G097064E79876N				cdef	adef	c-e		acdef		10
43	marine	411.1	G094682E80294N				abcdef	abcdef	a-b				9
67	land	24.7	G099506E79382N						a-c	acdef			8
38	marine	712.5	G094143E80332N					bcdef	b-f		bcdef		7
139	marine	168.1	G096735E80048N					ab	a-b		abcdef		7
143	marine	468.8	G096683E80578N					bcdef	d-e		bcdef		7
49	marine	196.5	G096576E80253N					abcdef	a-b				6
70	land	87.5	G098974E79688N	cdef	b								6
1	marine	120.6	G097867E80049N					a				acdef	5
137	marine	828.5	G096063E80433N				def	bdef			cdef		5
2	marine	275.4	G095561E80299N				aef	abcdef			c		5
31	land	93.3	G094665E79378N			f	f	f					5
77	land	511.3	G096205E79192N							c-f			5
104	land	419.0	G096481E79287N							c-f			5
154	land	103.8	G093581E80318N							d-f			5



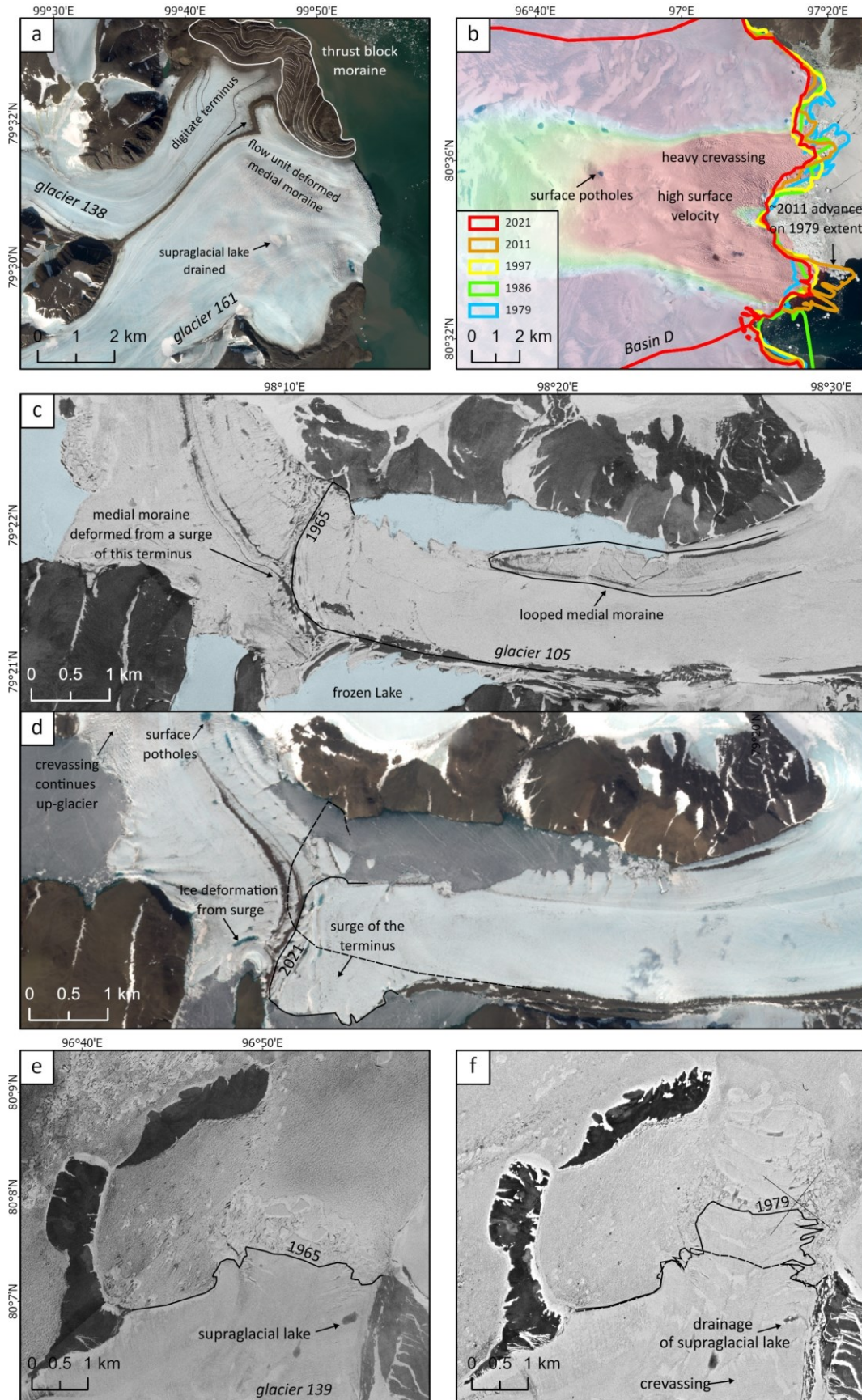
440 **Fig. 9.** Classification of glaciers by likelihood of being surge-type based on a systematic identification of each  
 441 glacier for surge-indicative features (see Table 1).

442

443 Evidence of surging predominantly occurs north of 79°N on October Revolution Island and  
 444 Komsomolets Island (Fig. 9). Surge-type glaciers (including category 2 - likely to have surged and  
 445 category 3 - possible surge-type) all originate from large ice caps, primarily clustered around the  
 446 Academy of Sciences Ice Cap, Rusanov Ice Cap and Karpinsky with no evidence of surging in the  
 447 Albanov, University Ice Cap or on Bolshevik Island. Glaciers with evidence of surging have a mean size

448 of 312 km<sup>2</sup> (median: 284.5 km<sup>2</sup>) compared to 86 km<sup>2</sup> for non-surge-type glaciers. All category 1 -  
449 confirmed surge-type glaciers are marine/lake terminating, although this is less prominent (65%)  
450 when category 2 - likely to have surged and category 3 - possible surge-type glaciers are included  
451 (Table 3).

452           Between 1965 and 2021, 10 localised abnormal advances (>0.5 km<sup>2</sup>) were observed at various  
453 times and of varying duration (see supplementary spreadsheet 1). The western margins of the Vavilov  
454 Ice Cap exhibited the largest advance between any date, extending ~11 km further into the Kara Sea  
455 than its position in 2011 (Fig. 5h). The surrounding basins of the Vavilov Ice Cap underwent a minor  
456 advance as the western margin surged. The highest confidence classification is glacier 105, a lake-  
457 terminating glacier, which is observed to actively surge between 1987 - 2011 and shows evidence of  
458 having formerly surged at least twice; the surge classification is strengthened by the presence of a  
459 looped medial moraine (Fig. 10c-d; Supplementary Video S2).



461 **Fig. 10.** Evidence of surge-type glaciers. (a) Glacier 138 (north) and 161 (south) on the eastern Karpinsky Ice Cap,  
462 including the presence of a deformed medial moraine and a thrust block moraine in contact with the ice-margin  
463 at the terminus of glacier 138. (b) Localised advance to the south of Basin D of the Academy of Sciences Ice Cap  
464 between 1979 and 2011, including heavy crevassing and surface potholes. (c) 1965 KH-7 imagery of glacier 105.  
465 The frozen lake is artificially coloured blue to aid visibility. Note the presence of a looped medial moraine. (d)  
466 2021 Sentinel-2A imagery of glacier 105. (e) 1965 KH-7 imagery of glacier 139. (f) KH-9 1979 imagery showing a  
467 rapid localised advance of the terminus of glacier 13.

468

469 Surging prior to 1965 is mainly recorded by preserved thrust block/glacitectonic composite  
470 moraines, which likely record numerous advances due to surging, primarily on eastern October  
471 Revolution Island (e.g., Fig. 10a), which is one of the few areas to contain extensive forelands of  
472 deformable sediment. There are no preserved moraines beyond the limit of the possible surge  
473 moraines, most of which are still in contact with the ice front. As the surge diagnostic nature of thrust  
474 block/glacitectonic composite moraines is not entirely unequivocal (cf. Sharp, 1985; 1988; Evans and  
475 Rea, 1999; 2003; Fitzsimons, 1996; 1997; 2003; Ingolfsson and others 2016), their presence in the  
476 absence of other surge criteria is not regarded as sufficient evidence for a classification of possible  
477 surge-type (category 3). On Bolshevik Island, four small cirque glaciers are not classified as surge-type  
478 despite potential thrust-block/glacitectonic composite moraines at their termini due to a possible,  
479 alternative, controlled moraine interpretation of such forms (Evans, 2009).

480

## 481 5. DISCUSSION

### 482 5.1. Glacier Change & Climatic Forcing

#### 483 5.1.1. Spatiotemporal Trends in Glacier Change

484 Our results show that almost all glaciers (96%) on Severnaya Zemlya have, overall, retreated between  
485 1965 and 2021 (Fig. 4; Table 2). The reduction in glacierised area is attributed to atmospheric warming,  
486 with annual average air temperature increases of ~2-3 °C (1936-2021) and an increase in warmer than  
487 average SSTs surrounding Severnaya Zemlya compared to the climate normal time period (1991 to  
488 2020) (Fig. 7; Fig. 8). Glaciers and ice caps have retreated the least in the north of Severnaya Zemlya,  
489 with retreat rates increasing along a southward gradient (Fig. 4; Table 2). Until 1997, glaciers on  
490 northern Severnaya Zemlya were relatively stable, whereas on southern Severnaya Zemlya, glacier  
491 retreat was observed between 1952 and 1975 from a comparison of cartographic maps and aerial  
492 photography (Govorukha and others, 1987). Rates of glacier retreat notably accelerated in all regions  
493 post-1997, correlating with the transition between the colder period of the 1950s-1990s and rapid  
494 warming at the end of the 20th century (Fig. 3; Fig. 7).

495           Between 1965 and 2021, the largest losses in glacier area occurred on Bolshevik Island (-  
496 14.1%), in the south of Severnaya Zemlya (Table 2). Retreat rates have increased between each time  
497 slice post-1997, peaking at  $-9.6 \text{ km}^2 \text{ a}^{-1}$  (2011 to 2021) and of a magnitude higher than retreat rates  
498 elsewhere on Severnaya Zemlya (Table 2). Bolshevik Island is influenced by warmer surface air  
499 temperatures and SSTs on the Kara Sea coast and receives the most precipitation on Severnaya  
500 Zemlya, but precipitation totals have slightly fallen between 1981 and 2022 (Fig. 8). The closest  
501 weather station to Bolshevik Island, Im. E. K. Fedorova, shows a clear increase in summer air  
502 temperatures, unlike Ostrov Golomjannyj on western Severnaya Zemlya which shows no trend of  
503 summer warming (Fig. 1; Fig. 7). Glacier mass balance is most strongly controlled by summer climate  
504 (Möller and Kohler, 2018) and when increased summer ablation is combined with a decrease in winter  
505 precipitation (Fig. 8e), glacier mass balance will become increasingly negative. This combination of  
506 summer atmospheric warming occurring at a magnitude higher than the rest of Severnaya Zemlya and  
507 no change or a slight decrease in mean annual precipitation on Bolshevik Island specifically, provides  
508 a likely explanation for the southwards increase in retreat rates. It should be noted that glaciers on  
509 Bolshevik Island are smaller, and retreat is likely to be greater in percentage terms than larger glaciers  
510 (cf. Stokes and others, 2018). However, 55% of the total 1965 to 2021 glacier area loss ( $-426 \text{ km}^2$ )  
511 occurred there, thus showing that retreat is occurring disproportionately towards the south.

512           Northwards, glaciers and ice caps on October Revolution Island (-3.0%, 1965-2021) have  
513 retreated at a slower rate than on Bolshevik Island (-14.1%, 1965-2021), but recent observations  
514 indicate more dramatic changes (Table 2). The region underwent slow but incremental retreat until  
515 2011 when the westernmost basin of the Vavilov Ice Cap underwent a rapid advance (Fig. 5h; Willis  
516 and others, 2018) and the Matusveich Ice Shelf collapsed (Fig. 6; Willis and others, 2015). Until its  
517 collapse, the Matusveich Ice Shelf was the largest floating ice shelf in the Russian High Arctic and had  
518 historically undergone cyclical terminus fluctuations due to large calving events and subsequent  
519 advances (Williams and Dowdeswell, 2001). In the three years preceding the collapse, summer  
520 temperatures were 1, 1 and 2 °C higher than normal, and one tributary glacier (Issledovateley)  
521 advanced, destabilising the Matusveich Ice Shelf and leading to its collapse in 2012 (Fig. 6; Willis and  
522 others, 2015). Post-collapse (2012 to 2014), a reduction in buttressing from the Matusveich Ice Shelf  
523 resulted in thinning rates that exceed the 30-year average rate for Severnaya Zemlya (Willis and  
524 others, 2018). By 2021, imagery shows that a large tabular iceberg from the breakup of the Khodov  
525 terminus remains grounded in Matusveich Fjord and former Matusveich Ice Shelf outlet glaciers show  
526 an increase in crevassing at their terminus (Fig. 6). Additionally, it is likely that the now exposed  
527 terminus of the Zhuravlev Glacier (Rusanov Ice Cap) is at risk of collapse from a lack of buttressing (Fig.

528 6). Due to warmer SSTs and a Severnaya Zemlya-wide pattern of retreat (1965 to 2021), a regeneration  
529 of the Matusевич Ice Shelf is deemed highly unlikely (Fig. 4; Fig. 8). The exposure of marine-  
530 terminating (Matusевич Ice Shelf-fed) outlet glaciers to warmer SSTs poses a risk of accelerated  
531 melting of the Rusanov and Karpinsky Ice Caps, which already have exhibited some of the highest rates  
532 of surface area loss on October Revolution Island.

533 Komsomolets Island (northernmost Severnaya Zemlya) shows the lowest overall change of  
534 the three main islands, having lost the least glacierised area between 1979 and 2021 (-1.9%; Table 2).  
535 The Academy of Sciences Ice Cap occupies most of Komsomolets Island and has had a mass balance  
536 close to zero for the last four decades (Bassford and others, 2006a; Sánchez-Gómez and others, 2019).  
537 However, between 1965 and 2021, two basins have increased in surface area and multiple basins of  
538 the Academy of Sciences Ice Cap show evidence of cyclical advance and retreat patterns (Moholdt and  
539 others, 2012b). The majority of advances observed in this study (from 1979 to 2021) are from one of  
540 the four fast-flowing Academy of Sciences Ice Cap 'ice streams', which have velocities of a magnitude  
541 higher than the rest of Severnaya Zemlya (Table 3). It is not known what causes these ice streams to  
542 advance, although it has been argued that their sub-glacial geology, if deformable, could support  
543 transient subglacial deformation, or that drainage of water to the bed could explain glacier speed-up  
544 events (Moholdt and others, 2012b). Hence, it is suggested here that this is a viable explanation, as  
545 the drainage and re-appearance of large meltwater lakes on most of the 'ice streams' is observed,  
546 which may route meltwater to the glacier bed and result in glacier speed-up events. These advances  
547 are unlikely to be primarily driven by climate as they are asynchronous and the ice cap's mass balance  
548 remains close to zero (Moholdt and others, 2012b; Navarro and others, 2020). Thus, it is most  
549 probable that the speed-up events are due to the characteristics of the ice cap or another mechanism  
550 (e.g., surging).

551 Overall, accelerated glacier retreat on Severnaya Zemlya is attributed to a 2-3 °C increase in  
552 mean annual surface air temperatures on the northern Taymyr Peninsula (the most proximal  
553 meteorological station to Bolshevik Island) and offshore from October Revolution Island (1936 to  
554 2021; Fig. 7a-b). The highest rates of retreat occurred at land-terminating glaciers on Bolshevik Island  
555 and are likely due to increasing summer atmospheric surface temperatures on the proximal Taymyr  
556 Peninsula (Fig. 7c). Summer warming is the primary control on glacier retreat, leading to increased  
557 ablation, which may be exacerbated by a lengthened melt season due to annual warming trends  
558 resulting in an increase in days above 0 °C, particularly in spring and autumn. Increased ablation, which  
559 on Bolshevik Island has not been counteracted by increased precipitation, has likely resulted in an  
560 increasingly negative glacier mass balance, which has manifested as a reduction in glacier surface area

561 (Fig. 8e-f). In contrast, further north there is no apparent trend in summer warming and the rate of  
562 precipitation (1936 to 2021) has remained steady or has increased (Fig. 7d; Fig. 8e-f). Although the  
563 melt season may have become longer in the north, retreat has occurred at a slower rate due to lower  
564 rates of summer warming and ablation compared to Bolshevik Island (Fig. 7c, Fig. 7f). Additionally,  
565 there is evidence that declining sea ice concentrations due to oceanic warming may allow for  
566 increased heat flux transfer from the ocean to the atmosphere (Rodrigues, 2008; Tepes and others,  
567 2021b), with a statistically significant correlation between reduced late-summer sea ice  
568 concentrations and earlier surface snowpack melt (Zhao and others, 2014). This trend in oceanic  
569 warming is attributed by Tepes and others (2021b) to be the primary driver of mass loss on Severnaya  
570 Zemlya. However, as the highest reductions in surface area are observed at land-terminating glaciers  
571 on Bolshevik Island, it is suggested that atmospheric warming is more influential than previously  
572 thought, especially on small, land-terminating glaciers in the south. It is anticipated that Severnaya  
573 Zemlya will become increasingly negative in mass balance as summer warming trends are likely to  
574 increase, whilst sea-ice concentrations are likely to decrease, resulting in higher rates of ablation that  
575 cannot be sustained by the current rates of precipitation.

576

#### 577 *5.1.2. Comparison to other Arctic regions*

578 The absence of summer warming trends in surface air temperature (1936 to 2021) on northern  
579 Severnaya Zemlya is in accordance with Novaya Zemlya (1990 to 2011) (Carr and others, 2014),  
580 although Novaya Zemlya has since become a hotspot for warm anomalies (2011 to 2016) (Ciraci and  
581 others, 2018). South of Severnaya Zemlya, the Taymyr peninsula on mainland Russia has seen an  
582 increase in positive summer air temperature anomalies, which may also have occurred on southern  
583 Severnaya Zemlya (Fig. 7c). Similar to Severnaya Zemlya, Svalbard exhibits a strong trend of winter  
584 warming ( $1.6\text{ }^{\circ}\text{C decade}^{-1}$ , 1961-2012) and, to a lesser degree, summer warming ( $0.2\text{ }^{\circ}\text{C decade}^{-1}$ , 1961-  
585 2012). The latter has been pinpointed as the key driver of glacier thinning on Svalbard and, when  
586 combined with the trend of declining summer precipitation, has resulted in glaciers experiencing a  
587 negative mass balance (van Pelt and others, 2016; Geyman and others, 2022). The warming trends  
588 and resulting glacier retreat observed in the western Barents-Kara region (i.e., Svalbard and western  
589 Novaya Zemlya) can be used as a predictor for the future glaciological changes on Severnaya Zemlya,  
590 as its warming is delayed with respect to the western Barents-Kara Sea region (Tepes and others,  
591 2021b).

592 Strong winter warming trends in the Barents Sea have been linked to sea ice decline and a  
593 subsequent acceleration of glacier retreat (Carr and others, 2014; Tepes and others, 2021b). In  
594 addition, the increased encroachment of warmer Atlantic waters into the Eurasian Basin has been  
595 attributed to changes in the Atlantic Multi-decadal Oscillation and North Atlantic Oscillation, leading  
596 to further sea ice decline (Carr and others, 2017b; Carvalho and Wang, 2020). There is also evidence  
597 that, in recent decades, Ural blocking events, which are blocking anticyclonic anomalies over the  
598 Eurasian subarctic region, have contributed to reduced sea ice concentrations and warmer air  
599 temperatures in the Barents-Kara Sea region (Luo and others, 2016; 2019). The strength of Ural  
600 blocking events has also been linked to different phases of El Niño-Southern Oscillation (ENSO), hence  
601 ENSO may be an additional driver of changing sea ice concentrations in the Eurasian Arctic (Luo and  
602 others, 2021). The effect of long-term sea ice decline has been observed in the Arctic, notably in  
603 Greenland, where retreat rates have increased during phases of low or no sea ice (Reeh and others,  
604 2001; Amundson and others, 2010; Moon and others, 2015). At present, sea ice concentrations have  
605 declined around Severnaya Zemlya, but still remain relatively high, and thus there is no difference in  
606 retreat rates (outside of error margins) between land and marine-terminating glaciers (Rodrigues,  
607 2008; Onarheim and others, 2018). In contrast, glacier retreat at marine-terminating outlets on  
608 neighbouring Novaya Zemlya and Franz Josef Land is observed to have occurred at a disproportionately  
609 faster rate compared to land-terminating glaciers (Carr and others, 2014; Moon and others, 2015;  
610 Zheng and others, 2018). On Novaya Zemlya, marine-terminating glaciers have retreated 3.5 times  
611 faster than land-terminating glaciers (Carr and others, 2017b). The results presented here show that  
612 the largest reductions in glacier surface area have occurred at land-terminating glaciers in the far  
613 south of Severnaya Zemlya (Fig. 4). Hence, we deduce that glacier retreat at land-terminating glaciers  
614 on southern Severnaya Zemlya is primarily driven by atmospheric and not oceanic warming. Marine-  
615 terminating glaciers are likely to respond in a more complex manner, in that their dynamics can be  
616 forced by both atmospheric and oceanic warming, along with changing sea-ice concentrations (Moon  
617 and others, 2015; Carr and others, 2017b). It is anticipated that under continued sea ice decline due  
618 to climatic warming over the next few decades, the magnitude of marine-terminating glacier retreat  
619 on Severnaya Zemlya is likely to greatly exceed that of land-terminating glaciers.

620

## 621 **5.2. Identification of Surge Type Glaciers**

### 622 *5.2.1. Occurrence*

623 Within the Russian High Arctic, glacier surging has been perceived to be confined to the more  
624 temperate climate of Novaya Zemlya (Grant and others, 2009). In contrast, predominantly cold-based

625 glaciers, as seen further east (e.g., Severnaya Zemlya), have not traditionally been associated with  
626 surge-type behaviour, despite some clear evidence to the contrary (e.g., Hattersley-Smith 1969;  
627 Copland and others 2003; Van Wychen and others, 2016). Models predict that surging may occur on  
628 Severnaya Zemlya and note the need for further investigation in the region (Sevestre and Benn, 2015).  
629 The notion that surging occurs on Severnaya Zemlya was supported by the identification of two looped  
630 medial moraines by Dowdeswell and Williams (1997) from 30 m imagery on the eastern Karpinsky Ice  
631 Cap. More recently, a large destabilisation of the western Vavilov Ice Cap in 2012 implied that surge-  
632 like behaviour may be more widespread on Severnaya Zemlya than previously thought (Willis and  
633 others, 2018). This ‘surge’, or more correctly “speed-up event”, shared similar properties to that of a  
634 large fast-flow event at Austfonna, Svalbard (Dunse and others, 2011; Gong and others, 2018) and  
635 numerous other active phases of surging observed in more temperate Svalbard. Contrary to the  
636 Svalbard polythermal glacier regime, glaciers on Severnaya Zemlya are thought to be predominantly  
637 cold-based and receive less precipitation, meaning the quiescent period is likely to be longer.  
638 However, given the presence of the looped medial moraines observed by Dowdeswell and Williams  
639 (1997), it is likely that surging has and does occur on Severnaya Zemlya, and this is confirmed in the  
640 present study. Indeed, it is proposed that surging is more widespread on Severnaya Zemlya than  
641 initially thought, with 20 glaciers possibly of surge-type (Table 3; Fig. 9). When sub-divided by  
642 confidence, three glaciers are classified as category 1 - confirmed surge-type, eight are category 2 -  
643 likely to have surged and nine are category 3 - possible surge-type. The recent availability of higher  
644 resolution imagery (e.g., ArcticDEM, 2 m, Sentinel-2A, 10m) and the use of multiple dates (1965, 1979,  
645 1986, 1999, 2011 & 2021) may partly explain the increased detection of surge-type glaciers compared  
646 to previous attempts (Dowdeswell and Williams, 1997).

647         There are fewer glaciers classified as surge-type on Severnaya Zemlya than on Novaya Zemlya  
648 and Svalbard, but compared to Novaya Zemlya, surge-type glaciers (including category 2 - likely to  
649 have surged and category 3 - possible surge-type) on Severnaya Zemlya occupy a disproportionate  
650 portion of its glacierised area. As a percentage of glacierised area and including both possible surge-  
651 type glaciers and likely to have surged, the 37% surge glacier coverage of Severnaya Zemlya exceeds  
652 that of Novaya Zemlya (~18%, including possible and likely to have surged; Grant and others, 2009),  
653 but is lower than Svalbard (~46.5%; Jiskoot and others, 1998). However, if we only include those  
654 classified as confirmed surge-type, the areal proportion is 8%. The difference in surge-type glacierised  
655 area between Severnaya Zemlya and Novaya Zemlya is attributed to many surge-type glaciers on  
656 Severnaya Zemlya being concentrated around the outlets of large ice domes, which are substantially  
657 larger than any ice cap on Novaya Zemlya. Overall, the number of surge-type glaciers decreases across

658 an eastward gradient from the surge climatically optimal region of Svalbard to Novaya Zemlya and  
659 Severnaya Zemlya (Sevestre and Benn, 2015).

660 It is probable that surging on Severnaya Zemlya occurs less frequently than further west due  
661 to Severnaya Zemlya's lower rates of precipitation, increasing the time required for glaciers to re-gain  
662 enough mass to surge. As precipitation is a control on the length of the quiescent period (Eisen and  
663 others, 2001), it makes identifying multiple surges unlikely in colder, dryer climates like Severnaya  
664 Zemlya. Traditional surge definitions state that advances must be cyclical for a glacier to be surge-  
665 type. Thus, without observing cyclical behaviour it cannot be confirmed whether externally forced  
666 one-off speed-up events rather than cyclical/repeated surges occur on Severnaya Zemlya. However,  
667 one glacier (105) is observed in its active phase (~1986 to 2010) and has a looped medial moraine in  
668 1965 imagery, which presumably formed before the active phase commenced. Hence, it is likely a relic  
669 from a prior surge, implying that the glacier has surged at least twice (Fig. 10c-d).

670 The presence of surge-indicative features is less common on Severnaya Zemlya than on  
671 Svalbard, with notable differences in foreland geomorphology. Any geomorphological record of  
672 surging on Severnaya Zemlya is likely represented by the superimposition of proglacial thrust masses  
673 as glacier extent has remained close to modern margins since the LGM (Raab and others, 2003),  
674 illustrated by the thrust block moraines on eastern October Revolution Island (Fig. 10a). Many glaciers  
675 remain in contact with thrust block moraines at their terminus, with no inner zone in which to identify  
676 other surge diagnostic forms such as long flutings, geometric ridge networks or zig-zag eskers (Evans  
677 and Rea, 2003; Ingólfsson and others, 2016). Where forelands are exposed, they contain no such clear  
678 evidence of glacier surging. A similar scenario occurs in the Canadian High Arctic where glaciers that  
679 have constructed thrust moraines are not traditionally interpreted as surge-type (cf. Evans and  
680 England, 1991; 1992; Copland and others, 2003; Ó Cofaigh and others, 1999; 2003). Consequently,  
681 future research needs to further investigate the landsystem imprint typical of cold-based glacier  
682 systems in order to assess the presence, both former and contemporary, of High Arctic glacier surges.

683

#### 684 *5.2.2. Distribution*

685 Surging on Severnaya Zemlya is primarily clustered around north-eastern Severnaya Zemlya, on the  
686 Academy of Sciences Ice Cap, Karpinsky and Rusanov Ice Caps (Fig. 9). Within these ice caps, individual  
687 basins classified as surge-type display no preferential aspect. The geomorphological imprint of surging  
688 is primarily clustered around the Karpinsky Ice Cap, in eastern Severnaya Zemlya, where glaciers  
689 descend from areas of higher elevation down to areas of deformable sediment on the Laptev Sea

690 coast. Glaciers on the Laptev Sea coast are more likely to be marine-terminating and this coastal zone  
691 is characterised by colder surface air temperatures and lower equilibrium line altitudes even though  
692 there are warmer SSTs on the continental shelf here than on the Kara Sea coast (Fig. 8a; Fig. 8c).  
693 However, it is clear that surging is not restricted to a climatic envelope on the Laptev Sea coast due to  
694 the ice-marginal speed-up event on the Vavilov Ice Cap and the post-surge geometry of Basin A, both  
695 of which are on the Kara Sea coast (Fig. 5a; Fig. 5h).

696 If warmer ice temperatures and polythermal glacier regimes increase the likelihood of glacier  
697 surging, surging should be most prevalent on the warmer, southernmost, Bolshevik Island, which  
698 contains small glaciers and ice caps. However, there is no explicit evidence of past surging on the  
699 island, with the exception of four small ( $\sim 0.5\text{-}1.5\text{ km}^2$ ) cirque glaciers that have disproportionately large  
700 ice-cored, potentially thrust-block, terminal moraines. Using our protocol, these glaciers are not  
701 classified as surge-type due to the absence of other surge-indicative features. These small cirques  
702 differ from the characteristics typical of surge-type glaciers on Severnaya Zemlya, Novaya Zemlya and  
703 on Svalbard, which are predominantly long, have relatively steep slopes and occupy larger basins  
704 (Jiskoot and others, 2000; Grant and others, 2009; Sevestre and Benn, 2015). However, small cirque  
705 glaciers have been observed to surge in northern Iceland (Brynjólfsson and others, 2012; Ingólfsson  
706 and others, 2016) and, despite differing basal thermal regimes between Iceland and Severnaya  
707 Zemlya, these glaciers may have once surged. Notwithstanding this evidence for possible surging  
708 cirque glaciers, there is a lack of unequivocal surging activity on Bolshevik Island.

709 The existence of surge-type glaciers on Komsomolets Island has been debated (e.g., Moholdt  
710 and others, 2012b). However, it is suggested that evidence is sufficient to assume that surging has  
711 most likely occurred in the Academy of Sciences Ice Cap. According to our protocol, within the  
712 Academy of Sciences Ice Cap, we classify three glaciers as category 2 - likely to have surged and four  
713 as category 3 - possible surge-type. Prior research has found no evidence of past surge activity within  
714 the residency time of the ice, in the form of looped medial moraines, heavy surface crevassing or rapid  
715 localised glacier advances (Dowdeswell and others, 2002). Previous studies (Moholdt and others,  
716 2012b; Sánchez-Gómez and others, 2019) and glacier change mapping from this study show that the  
717 ice streams of the Academy of Sciences Ice Cap (Basins B, BC, C, D) alternate between periods of slow  
718 and fast flow (e.g., Fig. 10b) (we classify them as likely to have surged, possible, possible, and likely to  
719 have surged, respectively). The mechanism driving this cyclical behaviour is unknown, but the notion  
720 that they are surge-type is supported by two basins (A & B) that have undergone surge-like elevation  
721 changes (Moholdt and others, 2012b) (we classify both as category 2 - likely to have surged). These  
722 changes were followed by a deceleration in ice flow velocity in Basin A, which is characterised by a

723 typical post-surge geometry (Moholdt and others, 2012b). In addition, we observe a small but steady  
724 advance of Basin A at the north-eastern margin of its low-gradient lobe and a small advance between  
725 1979-1997 at its terminus (Fig. 5a). Despite there being alternative explanations for the existence of  
726 some surge-indicative features (e.g., shear margins are also typical of ice streams), some features,  
727 such as the large low-gradient lobe characteristic of a post-surge terminus, are difficult to attribute to  
728 another mechanism (Fig. 5a). Thus, it is deemed likely that surging has occurred in the Academy of  
729 Sciences Ice Cap, but there is no chronological constraint on when it occurred.

730           Similar issues of equifinality exist when determining whether the glaciers that fed the former  
731 Matusevich Ice Shelf on October Revolution Island are of surge-type. Before its collapse in 2012, there  
732 was evidence of an acceleration in ice flow velocity in the ice shelf's tributary glaciers between 1965  
733 and 1995 (Sharov and others, 2015). As this velocity speed-up was synchronous with other glaciers  
734 this behaviour can be dismissed as surging. Additionally, observations show a notable localised  
735 advance of one tributary glacier (Issledovateley) between 1986 and 1997, which in conjunction with  
736 its heavy crevassing classifies this glacier as surge-type using our protocol (Fig. 6). Nevertheless, we  
737 suggest that this advance may not be due to surging *sensu stricto* as the ice shelf is known to undergo  
738 cyclical patterns of disintegration and re-establishment every 30 years (Williams and Dowdeswell,  
739 2001). As the last advance was between 1962 and 1973 (Willis and others, 2015), the advance  
740 recorded between 1986 and 1997 is ~30 years later and therefore appears to be part of the cyclical  
741 behaviour that drives speed-up events. Moreover, it is unlikely that a quiescent phase would be as  
742 short as ~30 years when such phases are typically 50 to 100 years in duration on Svalbard (Dowdeswell  
743 and others, 1991).

744

### 745           5.2.3. Characteristics

746 Surge-type glaciers are typically characterised by an imbalance whereby they are not able to efficiently  
747 regulate mass, resulting in a surge/quiescent cycle (Sevestre and Benn, 2015; Benn and others, 2019).  
748 Glacier length and slope appear to be the key differentiators between surge-type and non-surge-type  
749 glaciers, with surge-type glaciers most likely to be longer with shallower slope angles (Clarke and  
750 others, 1986; Jiskoot and others, 1998; Grant and others, 2009; Sevestre and Benn, 2015). Our results  
751 show that surging on Severnaya Zemlya is mainly restricted to long outlet glaciers descending from  
752 larger ice caps, notably around Mount Karpinsky, the highest point on Severnaya Zemlya (Fig. 9).  
753 Marine and lake-terminating glaciers are most likely to surge on Severnaya Zemlya and account for  
754 65% of glaciers classified as potential surge-type. However, the number of marine-terminating surge-

755 type glaciers may be underestimated due to the absence of bathymetric datasets, which would  
756 otherwise allow for the identification of landforms characteristic of the tidewater surge-type glacier  
757 landsystem model (Ottesen and others, 2008; Flink and others, 2015).

758 We assume that surge-type glaciers on Severnaya Zemlya are characterised by a longer  
759 quiescent and active surging phase than glaciers in warmer climates with higher rates of precipitation.  
760 The observation of active surging on glacier 105, for example, occurred for ~24 years between 1986  
761 to 2010 (Supplementary Video S2). Additionally, the surge of the Vavilov ice cap has continued for >10  
762 years post-destabilisation in 2011. In comparison, surges on Svalbard can be as short as 2 years (e.g.,  
763 Tunabreen) but may last longer than 10 years in some cases (e.g., Basin 3, Austfonna) (Dunse and  
764 others, 2015; Benn and others, 2023). If these slow advances on Severnaya Zemlya are due to surging,  
765 as assumed, the active phase duration may be similar to glaciers in the cold, dry Canadian High Arctic,  
766 where the active phase has exceeded 20-50 years for some glaciers (Copland and others, 2003; Van  
767 Wychen and others, 2016; Lauzon and others, 2023). Despite the fact that surging has not been  
768 observed with sufficient frequency to accurately constrain the duration of the active and quiescent  
769 phases, it can be assumed that the duration required for replenishing the mass to enable surging  
770 would take longer than in areas with higher rates of annual snowfall (e.g., Svalbard and Alaska) (Eisen  
771 and others, 2001; Harrison and others, 2008; Kochtitzky and others, 2020). Thus, it is suggested that  
772 surging occurs less frequently on Severnaya Zemlya than in areas westward towards the Barents Sea,  
773 where annual rates of snowfall are higher. Indeed, glaciers further west in the Barents Sea region may  
774 offer a useful analogue as to how glacier dynamics will change on SZ under increasing oceanic and  
775 atmospheric temperatures, which could affect the occurrence of surging. At some temperate and  
776 polythermal glaciers in the Yukon, Canada and on Svalbard, increased temperatures may have resulted  
777 in a reduction in surging due to insufficient mass to surge (e.g., Małecki and others, 2013; Kochtitzky  
778 and others, 2020), whereas for cold-based glaciers, the transition to a polythermal regime may  
779 increase surging (e.g., Willis and others, 2018). Under continued warming, we anticipate accelerated  
780 retreat and increased likelihood of surging on Severnaya Zemlya as basal thermal regimes shift from  
781 predominantly cold-based to polythermal/warm-based.

782

## 783 **6. CONCLUSIONS**

784 This study finds that Severnaya Zemlya has undergone substantial surface area loss (-778 km<sup>2</sup>, -5%)  
785 from 1965 (17,053 ± 38 km<sup>2</sup>) to 2021 (16,275 ± 69 km<sup>2</sup>) and shows increasing evidence of glacier  
786 response to climatic warming. Spatiotemporal trends show that glacier retreat has accelerated post-

787 1997, with retreat mostly concentrated around land-terminating glaciers on southernmost Severnaya  
788 Zemlya (Bolshevik Island). We attribute higher rates of retreat southwards to increased evidence of  
789 summer atmospheric warming, which is not yet evident in northern Severnaya Zemlya. As land-  
790 terminating glaciers also retreated in the north, albeit to a lesser degree, it is probable that annual  
791 atmospheric warming has lengthened the melt season. In addition to oceanic warming, which has  
792 previously been identified as a driver of glacier retreat on Severnaya Zemlya (Tepes and others,  
793 2021b), we suggest that atmospheric warming is also playing a key role.

794 Building upon the previous identification of two potential surge-type glaciers for the area and  
795 the destabilisation of the Vavilov Ice Cap (Dowdeswell and Williams, 1997; Willis and others, 2018),  
796 our findings suggest that surging is more common on Severnaya Zemlya than previously thought. Most  
797 glaciers are not surge-type, but we confirm that three glaciers out of 190 glaciers on Severnaya Zemlya  
798 are surge-type (Category 1: 1.6%), eight are likely to have surged (Category 2: 4.2%) and nine are  
799 possible surge-type (Category 3: 4.7%). Although small by number, these three categories represent  
800 37% of the glacierised area of Severnaya Zemlya, or 8% if only confirmed surge-type glaciers are  
801 included. Surge-type glaciers on Severnaya Zemlya occupy large, long, marine or lake-terminating  
802 basins and are primarily concentrated around the Karpinsky Ice Cap. The quiescent phase is assumed  
803 to be longer than Novaya Zemlya and Svalbard due to lower rates of precipitation, a colder climate,  
804 and the observation of only three active surge phases between 1965 and 2021 on glaciers confirmed  
805 as surge-type. From the three active phases observed, we suggest that the active phase of surging on  
806 Severnaya Zemlya is also longer than average, but further observation and monitoring of these glaciers  
807 is required.

808 Under continued amplification of Arctic warming, we anticipate accelerated rates of mass loss  
809 from the Russian High Arctic. On Severnaya Zemlya, climatic warming is likely to result in increasingly  
810 negative glacier mass balance. A transition from mostly cold-based thermal regimes to polythermal is  
811 also probable, together with increased surface melting and the potential for increased accumulation,  
812 which may result in a change in glacier dynamics on Severnaya Zemlya. This may result in the  
813 destabilisation of larger ice caps and increased surge-like behaviour that could increase the rate of sea  
814 level rise from the Russian High Arctic.

815

## 816 **SUPPLEMENTARY MATERIAL**

817 Supplementary material accompanies the online version of this manuscript.

818

819 **ACKNOWLEDGEMENTS**

820 This research was carried out as part of a Masters by Research in the Department of Geography at  
821 Durham University. Data produced by this study will be submitted to the GLIMS Glacier Database. We  
822 thank Harold Lovell and an anonymous reviewer for constructive comments on an earlier version of  
823 this manuscript, together with the Scientific Editor, Neil Glasser, and Chief Editor, Hester Jiskoot. Dave  
824 Roberts is also thanked for comments on an earlier draft of this work.

825

826 **7. References**

- 827 Amundson JM, Fahnestock M, Truffer M, Brown J, Lüthi MP and Motyka RJ (2010) Ice mélange  
828 dynamics and implications for terminus stability, Jakobshavn Isbræ, Greenland. *Journal of*  
829 *Geophysical Research: Earth Surface*, **115**(F1) (doi: 10.1029/2009JF001405)
- 830 Andreev AA and Klimanov VA (2000) Quantitative Holocene climatic reconstruction from Arctic  
831 Russia. *Journal of Paleolimnology*, **24**(1), 81-91 (doi: 10.1023/A:1008121917521)
- 832 Bamber JL, Oppenheimer M, Kopp RE, Aspinall WP and Cooke RM (2019) Ice sheet contributions to  
833 future sea-level rise from structured expert judgment. *Proceedings of the National Academy*  
834 *of Sciences*, **116**(23), 11195-11200 (doi: 10.1073/pnas.1817205116)
- 835 Bassford RP, Siegert MJ, Dowdeswell JA, Oerlemans J, Glazovsky AF and Macheret YY (2006a)  
836 Quantifying the mass balance of ice caps on Severnaya Zemlya, Russian High Arctic. I:  
837 Climate and mass balance of the Vavilov Ice Cap. *Arctic, Antarctic, and Alpine*  
838 *Research*, **38**(1), 1-12 (doi: 10.1657/1523-0430(2006)038[0001:QTMBOI]2.0.CO;2)
- 839 Bassford RP, Siegert MJ and Dowdeswell JA (2006b) Quantifying the mass balance of ice caps on  
840 Severnaya Zemlya, Russian High Arctic. II: Modeling the flow of the Vavilov Ice Cap under the  
841 present climate. *Arctic, Antarctic, and Alpine Research*, **38**(1), 13-20 (doi: 10.1657/1523-  
842 0430(2006)038[0013:QTMBOI]2.0.CO;2)
- 843 Bassford RP, Siegert MJ and Dowdeswell JA (2006c) Quantifying the mass balance of ice caps on  
844 Severnaya Zemlya, Russian High Arctic. III: Sensitivity of ice caps in Severnaya Zemlya to  
845 future climate change. *Arctic, Antarctic, and Alpine Research*, **38**(1), 21-33 (doi:  
846 10.1657/15230430(2006)038[0021:QTMBOI]2.0.CO;2)
- 847 Benn DI and Evans DJA (2010) *Glaciers and Glaciation*, 2nd edn. Hodder, London.
- 848 Benn DI, Fowler AC, Hewitt I and Sevestre H (2019) A general theory of glacier surges. *Journal of*  
849 *Glaciology*, **65**(253), 701-716 (doi: 10.1017/jog.2019.62)
- 850 Benn DI, Hewitt IJ and Luckman AJ (2023) Enthalpy balance theory unifies diverse glacier surge  
851 behaviour. *Annals of Glaciology*, 1-7 (doi: 10.1017/aog.2023.23)
- 852 Brynjólfsson S, Ingólfsson Ó and Schomacker A (2012) Surge fingerprinting of cirque glaciers at the  
853 Tröllaskagi peninsula, North Iceland. *Jökull*, **62**(1), 151-166.

- 854 Carr JR, Stokes CR and Vieli A (2014) Recent retreat of major outlet glaciers on Novaya Zemlya,  
855 Russian Arctic, influenced by fjord geometry and sea-ice conditions. *Journal of*  
856 *Glaciology*, **60**(219), 155-170 (doi: 10.3189/2014JoG13J122)
- 857
- 858 Carr JR, Stokes CR and Vieli A (2017a). Threefold increase in marine-terminating outlet glacier retreat  
859 rates across the Atlantic Arctic: 1992–2010. *Annals of Glaciology*, **58**(74), 72-91 (doi:  
860 10.1017/aog.2017.3)
- 861 Carr JR, Bell H, Killick R and Holt T (2017b) Exceptional retreat of Novaya Zemlya's marine-  
862 terminating outlet glaciers between 2000 and 2013. *The Cryosphere*, **11**(5), 2149-2174 (doi:  
863 10.5194/tc-11-2149-2017)
- 864 Carvalho KS and Wang S (2020). Sea surface temperature variability in the Arctic Ocean and its  
865 marginal seas in a changing climate: Patterns and mechanisms. *Global and Planetary*  
866 *Change*, **193**(103265) (doi: 10.1016/j.gloplacha.2020.103265)
- 867 Chen JL, Wilson CR and Tapley BD (2013) Contribution of ice sheet and mountain glacier melt to  
868 recent sea level rise. *Nature Geoscience*, **6**(7), 549-552 (doi: 10.1038/ngeo1829)
- 869 Cherezova AA and 9 others (2020) Lateglacial and Holocene palaeoenvironments on Bolshevik Island  
870 (Severnaya Zemlya), Russian High Arctic. *Boreas*, **49**(2), 375-388 (doi: 10.1111/bor.12428)
- 871 Ciraci E, Velicogna I. and Sutterley TC (2018) Mass balance of Novaya Zemlya archipelago, Russian  
872 High Arctic, using time-variable gravity from grace and altimetry data from ICESat and  
873 Cryosat-2. *Remote Sensing*, **10**(11) (doi: 10.3390/rs10111817)
- 874 Ciraci E, Velicogna I and Swenson S (2020) Continuity of the mass loss of the world's glaciers and ice  
875 caps from the GRACE and GRACE Follow-On missions. *Geophysical Research Letters*, **47**(9)  
876 (doi: 10.1029/2019GL086926)
- 877 Clarke GKC, Schmok JP, Ommanney CSL and Collins SG (1986) Characteristics of surge-type glaciers.  
878 *Journal of Geophysical Research: Solid Earth*, **91**(B7), 7165-7180 (doi:  
879 10.1029/JB091iB07p07165).
- 880 Cook AJ and 7 others (2019) Atmospheric forcing of rapid marine-terminating glacier retreat in the  
881 Canadian Arctic Archipelago. *Science Advances*, **5**(3), eaau8507 (doi:  
882 10.1126/sciadv.aau8507)
- 883 Copland L., Sharp MJ and Dowdeswell JA (2003) The distribution and flow characteristics of surge-  
884 type glaciers in the Canadian High Arctic. *Annals of Glaciology*, **36**, 73-81 (doi:  
885 10.3189/172756403781816301)
- 886 DeBeer CM and Sharp MJ (2007) Recent changes in glacier area and volume within the southern  
887 Canadian Cordillera. *Annals of Glaciology*, **46**, 215-221 (doi: 10.3189/172756407782871710)
- 888 Dowdeswell JA and Williams M (1997) Surge-type glaciers in the Russian High Arctic identified from  
889 digital satellite imagery. *Journal of Glaciology*, **43**(145), 489-494 (doi:  
890 10.3189/S0022143000035097)

- 891 Dowdeswell JA, Hamilton GS and Hagen JO (1991) The duration of the active phase on surge-type  
892 glaciers: contrasts between Svalbard and other regions. *Journal of Glaciology*, **37**(127), 388-  
893 400 (doi: 10.3189/S0022143000005827)
- 894 Dowdeswell JA and 10 others (2002) Form and flow of the Academy of Sciences Ice Cap, Severnaya  
895 Zemlya, Russian High Arctic. *Journal of Geophysical Research: Solid Earth*, **107**(B4) (doi:  
896 10.1029/2000JB000129)
- 897 Dunse T, Greve R, Schuler TV and Hagen JO (2011) Permanent fast flow versus cyclic surgebehaviour:  
898 numerical simulations of the Austfonna ice cap, Svalbard. *Journal of Glaciology*, **57**(202),  
899 247-259 (doi: 10.3189/002214311796405979)
- 900 Dunse T, Schellenberger T, Hagen JO, Kääh A, Schuler TV and Reijmer H (2015) Glacier-surge  
901 mechanisms promoted by a hydro-thermodynamic feedback to summer melt. *The*  
902 *Cryosphere*, **9**(1), 197-215 (doi: 10.5194/tc-9-197-2015)
- 903 Edwards TL and 10 others (2021) Projected land ice contributions to twenty-first-century sea level  
904 rise. *Nature*, **593**(7857), 74-82 (doi: 10.1038/s41586-021-03302-y)
- 905 Eisen O, Harrison WD and Raymond CF (2001) The surges of Variegated Glacier, Alaska, USA, and  
906 their connection to climate and mass balance. *Journal of Glaciology*, **47**(158), 351-358 (doi:  
907 10.3189/172756501781832179)
- 908 Evans DJA (2009) Controlled moraines: origins, characteristics and palaeoglaciological implications.  
909 *Quaternary Science Reviews*, **28**(3-4), 183-208 (doi: 10.1016/j.quascirev.2008.10.024)
- 910 Evans DJA and England J (1991) Canadian Landform Examples - 19: High arctic thrust block moraines.  
911 *Canadian Geographer*, **35**, 93-97 (doi: 10.1111/j.1541-0064.1991.tb01628.x)
- 912 Evans DJA. and England J (1992) Geomorphological evidence of Holocene climatic change from  
913 northwest Ellesmere Island, Canadian high arctic. *The Holocene*, **2**(2), 148-158 (doi:  
914 10.1177/095968369200200)
- 915 Evans DJA and Rea BR (1999) Geomorphology and sedimentology of surging glaciers: a land-systems  
916 approach. *Annals of Glaciology*, **28**, 75-82 (doi: 10.3189/172756499781821823)
- 917 Evans DJA and Rea BR (2003) Surging glacier landsystem. In: Evans, D.J.A. (ed.), *Glacial Landsystems*.  
918 Arnold, London, 259-288.
- 919 Fitzsimons SJ (1996) Formation of thrust-block moraines at the margins of dry-based glaciers, south  
920 Victoria Land, Antarctica. *Annals of Glaciology*, **22**, 68-74 (doi: 10.3189/1996AoG22-1-68-74)
- 921 Fitzsimons SJ (1997) Glaciotectonic deformation of glaciomarine sediments and formation of thrust  
922 block moraines at the margin of an outlet glacier, Vestfold Hills, East Antarctica. *Earth*  
923 *Surface Processes and Landforms*, **22**, 175-187.
- 924 Fitzsimons SJ (2003) Ice-marginal terrestrial landsystems: polar continental glacier margins. In:  
925 Evans, D.J.A. (ed.), *Glacial Landsystems*. Arnold, London, 89-110.
- 926 Flink AE, Noormets R, Kirchner N, Benn DI, Luckman A and Lovell H (2015) The evolution of a  
927 submarine landform record following recent and multiple surges of Tunabreen glacier,  
928 Svalbard. *Quaternary Science Reviews*, **108**, 37-50 (doi: 10.1016/j.quascirev.2014.11.006)

- 929 Forman SL and 6 others (1999) Postglacial emergence and late Quaternary glaciation on northern  
930 Novaya Zemlya, Arctic Russia. *Boreas*, **28**(1), 133-145 (doi: 10.1111/j.1502-  
931 3885.1999.tb00210.x)
- 932 Fowler AC, Murray T and Ng FSL (2001) Thermally controlled glacier surging. *Journal of Glaciology*,  
933 **47**(159), 527-538. (doi: 10.3189/172756501781831792)
- 934 Geyman EC, van Pelt WJJ, Maloof AC, Aas HF and Kohler J (2022) Historical glacier change on  
935 Svalbard predicts doubling of mass loss by 2100. *Nature*, **601**(7893), 374-379 (doi:  
936 10.1038/s41586-021-04314-4)
- 937 Glazovsky A, Bushueva I and Nosenko G (2015) Slow 'surge' of the Vavilov Ice Cap, Severnaya  
938 Zemlya. *Proceedings of the IASC Workshop on the Dynamics and Mass Balance of Arctic*  
939 *Glaciers, Obergurgl, Austria, 23-25 March 2015* (from <https://nag.iasc.info/publications>, last  
940 accessed on 27<sup>th</sup> June 2023)
- 941 Gong Y and 6 others (2018) Simulating the roles of crevasse routing of surface water and basal  
942 friction on the surge evolution of Basin 3, Austfonna ice cap. *The Cryosphere*, **12**(5), 1563-  
943 1577 (doi: 10.5194/tc-12-1563-2018)
- 944 Govorukha LS, Bol'shiyanov DY, Zarkhidze VS, Pinchuk LY and Yunak RI (1987) Changes in the glacier  
945 cover of Severnaya Zemlya in the twentieth century. *Polar Geography and Geology*, **11**(4),  
946 300-305 (doi: 10.1080/10889378709377340)
- 947 Grant KL, Stokes CR and Evans IS (2009) Identification and characteristics of surge-type glaciers on  
948 Novaya Zemlya, Russian Arctic. *Journal of Glaciology*, **55**(194), 960-972 (doi:  
949 10.3189/002214309790794940)
- 950 Grosval'd MG and Kotlyakov VM (1969) Present-day glaciers in the USSR and some data on their  
951 mass balance. *Journal of Glaciology*, **8**(52), 9-22 (doi: 10.3189/S0022143000020748)
- 952 Hattersley-Smith G (1969) Recent observations on the surging Otto Glacier, Ellesmere Island.  
953 *Canadian Journal of Earth Sciences*, **6**, 883-889 (doi: 10.1139/e69-090)
- 954 Harrison WD and 7 others (2008) Another surge of variegated glacier, Alaska, USA, 2003/04. *Journal*  
955 *of Glaciology*, **54**(184), 192-194 (doi: 10.3189/002214308784409134)
- 956 Hewitt K (2007) Tributary glacier surges: an exceptional concentration at Panmah Glacier, Karakoram  
957 Himalaya. *Journal of Glaciology*, **53**(181), 181-188 (doi: 10.3189/172756507782202829)
- 958 Hubberten HW and 10 others (2004) The periglacial climate and environment in northern Eurasia  
959 during the Last Glaciation. *Quaternary Science Reviews*, **23**(11-13), 1333-1357 (doi:  
960 10.1016/j.quascirev.2003.12.012)
- 961 Hughes AL, Gyllencreutz R, Lohne ØS, Mangerud J and Svendsen JI (2016) The last Eurasian ice  
962 sheets—a chronological database and time-slice reconstruction, DATED-1. *Boreas*, **45**(1), 1-45  
963 (doi: 10.1111/bor.12142)
- 964 Ingólfsson Ó and 7 others (2016) Glacial geological studies of surge-type glaciers in Iceland—  
965 Research status and future challenges. *Earth-Science Reviews*, **152**, 37-69 (doi:  
966 10.1016/j.earscirev.2015.11.008)

- 967 Jiskoot H, Boyle P and Murray T (1998) The incidence of glacier surging in Svalbard: evidence from  
 968 multivariate statistics. *Computers & Geosciences*, **24**(4), 387-399 (doi: 10.1016/S0098-  
 969 3004(98)00033-8)
- 970 Jiskoot H, Murray T and Boyle P (2000) Controls on the distribution of surge-type glaciers in  
 971 Svalbard. *Journal of Glaciology*, **46**(154), 412-422 (doi: 10.3189/172756500781833115)
- 972 Kalnay E and 10 others (1996) The NCEP/NCAR 40-year reanalysis project. *Bulletin of the American  
 973 Meteorological Society*, **77**(3), 437-472 (doi: 10.1175/1520-  
 974 0477(1996)077<0437:TNYRP>2.0.CO;2)
- 975 Kamb B and 7 others (1985) Glacier surge mechanism: 1982-1983 surge of Variegated Glacier,  
 976 Alaska. *Science*, **227**(4686), 469-479 (doi: 10.1126/science.227.4686.469)
- 977 Khromova T, Nosenko G, Kutuzov S, Muraviev A and Chernova L (2014) Glacier area changes in  
 978 Northern Eurasia. *Environmental Research Letters*, **9**(1), 015003 (doi: 10.1088/1748-  
 979 9326/9/1/015003)
- 980 Khromova TE and 6 others (2021) New Catalog of Russian Glaciers Based on Satellite Data (2016–  
 981 2019). *Ice and Snow*, **61**(3), 341-358 (doi: 10.31857/S2076673421030093)
- 982 Kochtitzky W and 9 others (2020) Climate and surging of Donjek glacier, Yukon, Canada. *Arctic,  
 983 Antarctic, and Alpine Research*, **52**(1), 264-280 (doi: 10.1080/15230430.2020.1744397)
- 984 Lauzon B, Copland L, Van Wychen W, Kochtitzky W, McNabb R and Dahl-Jensen D (2023) Dynamics  
 985 throughout a complete surge of Iceberg Glacier on western Axel Heiberg Island, Canadian  
 986 High Arctic. *Journal of Glaciology*, 1-18 (doi: 10.1017/jog.2023.20)
- 987 Lawson W (1996) Structural evolution of variegated Glacier, Alaska, USA, since 1948. *Journal of  
 988 Glaciology*, **42**(141), 261-270 (doi: 10.3189/S0022143000004123)
- 989 Leigh JR, Stokes CR, Carr RJ, Evans IS, Andreassen LM and Evans DJA (2019) Identifying and mapping  
 990 very small (< 0.5 km<sup>2</sup>) mountain glaciers on coarse to high-resolution imagery. *Journal of  
 991 Glaciology*, **65**(254), 873-888 (doi: 10.1017/jog.2019.50)
- 992 Lubinski DJ, Forman SL and Miller GH (1999) Holocene glacier and climate fluctuations on Franz Josef  
 993 Land, Arctic Russia, 80 N. *Quaternary Science Reviews*, **18**(1), 85-108 (doi: 10.1016/S0277-  
 994 3791(97)00105-4)
- 995 Luo B, Wu L, Luo D, Dai A and Simmonds I (2019) The winter midlatitude-Arctic interaction: effects of  
 996 North Atlantic SST and high-latitude blocking on Arctic sea ice and Eurasian cooling. *Climate  
 997 dynamics*, **52**(5), 2981-3004 (doi: 10.1007/s00382-018-4301-5)
- 998 Luo B, Luo D, Dai A, Simmonds I and Wu, L (2021) A connection of winter Eurasian cold anomaly to  
 999 the modulation of Ural blocking by ENSO. *Geophysical Research Letters*, **48**(17),  
 1000 e2021GL094304 (doi: 10.1029/2021GL094304)
- 1001 Luo D, Xiao Y, Yao Y, Dai A, Simmonds I and Franzke CL (2016) Impact of Ural blocking on winter  
 1002 warm Arctic–cold Eurasian anomalies. Part I: Blocking-induced amplification. *Journal of  
 1003 Climate*, **29**(11), 3925-3947 (doi: 10.1175/JCLI-D-15-0611.1)

- 1004 Małecki J, Faucherre S and Strzelecki M (2013) Post- surge geometry and thermal structure of  
 1005 Hørbyebreen, central Spitsbergen. *Polish Polar Research*, **34**(3), 305- 321 (doi:  
 1006 10.2478/popore-2013-0019)
- 1007 Meier MF and Post AS (1969) What are glacier surges? *Canadian Journal of Earth Sciences*, **6**, 807-  
 1008 819 (doi: 10.1139/e69-081)
- 1009 Mengel M, Levermann A, Frieler K, Robinson A, Marzeion B and Winkelmann R (2016) Future sea  
 1010 level rise constrained by observations and long-term commitment. *Proceedings of the  
 1011 National Academy of Sciences*, **113**(10), 2597-2602 (doi: 10.1073/pnas.1500515113)
- 1012 Moholdt G, Wouters B and Gardner AS (2012a) Recent mass changes of glaciers in the Russian High  
 1013 Arctic. *Geophysical Research Letters*, **39**(10) (doi: 10.1029/2012GL051466)
- 1014 Moholdt G, Heid T, Benham T and Dowdeswell JA (2012b) Dynamic instability of marine-terminating  
 1015 glacier basins of Academy of Sciences Ice Cap, Russian High Arctic. *Annals of  
 1016 Glaciology*, **53**(60), 193-201 (doi: 10.3189/2012AoG60A117)
- 1017 Moon T, Joughin I and Smith B (2015) Seasonal to multiyear variability of glacier surface velocity,  
 1018 terminus position, and sea ice/ice mélange in northwest Greenland. *Journal of Geophysical  
 1019 Research: Earth Surface*, **120**(5), 818-833 (doi: 10.1002/2015JF003494)
- 1020 Moon T, Ahlstrøm A, Goelzer H, Lipscomb W and Nowicki S (2018) Rising oceans guaranteed: Arctic  
 1021 land ice loss and sea level rise. *Current Climate Change Reports*, **4**(3), 211-222 (doi:  
 1022 10.1007/s40641-018-0107-0)
- 1023 Möller M and Kohler J (2018) Differing climatic mass balance evolution across Svalbard glacier  
 1024 regions over 1900–2010. *Frontiers in Earth Science*, **6**, (doi: 10.3389/feart.2018.00128)
- 1025 Navarro FJ, Sánchez-Gómez P, Glazovsky AF and Recio-Blitz C (2020) Surface-elevation changes and  
 1026 mass balance of the Academy of Sciences Ice Cap, Severnaya Zemlya. *Ice and Snow*, **60**(1)  
 1027 (doi: 10.31857/S2076673420010021)
- 1028 Nela BR and 6 others (2019) Glacier flow dynamics of the Severnaya Zemlya archipelago in Russian  
 1029 high arctic using the differential SAR interferometry (DInSAR) technique. *Water*, **11**(12) (doi:  
 1030 10.3390/w11122466)
- 1031 Niessen F and 10 others (2013) Repeated Pleistocene glaciation of the East Siberian continental  
 1032 margin. *Nature Geoscience*, **6**(10), 842-846 (doi: 10.1038/ngeo1904)
- 1033 Noël B, van de Berg WJ, Lhermitte S, Wouters B, Schaffer N and van den Broeke MR (2018) Six  
 1034 decades of glacial mass loss in the Canadian Arctic Archipelago. *Journal of Geophysical  
 1035 Research: Earth Surface*, **123**(6), 1430-1449 (doi: 10.1029/2017JF004304)
- 1036 Ó Cofaigh C, Lemmen DS, Evans DJA and Bednarski J (1999) Glacial landform-sediment assemblages  
 1037 in the Canadian high arctic and their implications for late Quaternary glaciation. *Annals of  
 1038 Glaciology*, **28**, 195-201 (doi: 10.3189/172756499781821760)
- 1039 Ó Cofaigh C, Evans DJA and England J (2003) Ice marginal terrestrial landsystems: sub-polar glacier  
 1040 margins of the Canadian and Greenland high arctic. In: Evans D.J.A. (ed.), *Glacial Landsystems*.  
 1041 Arnold, London, 44-64.

- 1042 Onarheim IH, Eldevik T, Smedsrud LH and Stroeve JC (2018) Seasonal and regional manifestation of  
1043 Arctic sea ice loss. *Journal of Climate*, **31**(12), 4917-4932 (doi: 10.1175/JCLI-D-17-0427.1)
- 1044 Opel T, Fritzsche D and Meyer H (2013) Eurasian Arctic climate over the past millennium as recorded  
1045 in the Akademii Nauk ice core (Severnaya Zemlya). *Climate of the Past*, **9**(5), 2379-2389 (doi:  
1046 10.5194/cp-9-2379-2013)
- 1047 Ottesen D and 9 others (2008) Submarine landforms characteristic of glacier surges in two  
1048 Spitsbergen fjords. *Quaternary Science Reviews*, **27**(15-16), 1583-1599 (doi:  
1049 10.1016/j.quascirev.2008.05.007)
- 1050 Paul F (2015) Revealing glacier flow and surge dynamics from animated satellite image sequences:  
1051 examples from the Karakoram. *The Cryosphere*, **9**(6), 2201-2214 (doi: 10.5194/tc-9-2201-  
1052 2015)
- 1053 Polyak L, Niessen F, Gataullin V and Gainanov V (2008) The eastern extent of the Barents–Kara ice  
1054 sheet during the Last Glacial Maximum based on seismic-reflection data from the eastern  
1055 Kara Sea. *Polar Research*, **27**(2), 162-172 (doi: 10.1111/j.1751-8369.2008.00061.x)
- 1056 Polyakov IV and 10 others (2017) Greater role for Atlantic inflows on sea-ice loss in the Eurasian  
1057 Basin of the Arctic Ocean. *Science*, **356**(6335), 285-291 (doi: 10.1126/science.aai8204)
- 1058 Pörtner H-O and 100 others (2022) Technical Summary In: Climate Change 2022: Impacts,  
1059 Adaptation, and Vulnerability. Contribution of Working Group II to the Sixth Assessment  
1060 Report of the Intergovernmental Panel on Climate Change. Cambridge University Press. In  
1061 Press.
- 1062 Quincey DJ, Braun M, Glasser NF, Bishop MP, Hewitt K and Luckman A (2011) Karakoram glacier  
1063 surge dynamics. *Geophysical Research Letters*, **38**(18) (doi: 10.1029/2011GL049004)
- 1064 Raab A, Melles M, Berger GW, Hagedorn B and Hubberten HW (2003) Non-glacial  
1065 paleoenvironments and the extent of Weichselian ice sheets on Severnaya Zemlya, Russian  
1066 High Arctic. *Quaternary Science Reviews*, **22**(21-22), 2267-2283 (doi: 10.1016/S0277-  
1067 3791(03)00139-2)
- 1068 Rantanen M and 7 others (2022) The Arctic has warmed nearly four times faster than the globe since  
1069 1979. *Communications Earth & Environment*, **3**(1) (doi: 10.1038/s43247-022-00498-3)
- 1070 Raymond CF (1987) How do glaciers surge? A review. *Journal of Geophysical Research: Solid Earth*,  
1071 **92**(B9), 9121-9134 (doi: 10.1029/JB092iB09p09121)
- 1072 Reeh N, Thomsen HH, Higgins AK and Weidick A (2001) Sea ice and the stability of north and  
1073 northeast Greenland floating glaciers. *Annals of Glaciology*, **33**, 474-480  
1074 (doi:10.3189/172756401781818554)
- 1075 RGI Consortium (2017) Randolph Glacier Inventory - A Dataset of Global Glacier Outlines, Version  
1076 6.0. Boulder, Colorado USA. NSIDC: National Snow and Ice Data Center. (doi: 10.7265/4m1f-  
1077 gd79)
- 1078 Rodrigues J (2008) The rapid decline of the sea ice in the Russian Arctic. *Cold Regions Science and  
1079 Technology*, **54**(2), 124-142 (doi: 10.1016/j.coldregions.2008.03.008)

- 1080 Sánchez-Gómez P, Navarro FJ, Benham TJ, Glazovsky AF, Bassford RP and Dowdeswell JA (2019)  
 1081 Intra-and inter-annual variability in dynamic discharge from the Academy of Sciences Ice  
 1082 Cap, Severnaya Zemlya, Russian Arctic, and its role in modulating mass balance. *Journal of*  
 1083 *Glaciology*, **65**(253), 780-797 (doi: 10.1017/jog.2019.58)
- 1084 Sánchez-Gómez P, Navarro FJ, Dowdeswell JA, De Andrés E (2020) Surface velocities and calving flux  
 1085 of the Academy of Sciences Ice Cap, Severnaya Zemlya. *Ice and Snow*. **60**(1). 19-28 (doi:  
 1086 10.31857/S2076673420010020)
- 1087 Schauer U, Loeng H, Rudels B, Ozhigin VK and Dieck W (2002) Atlantic water flow through the  
 1088 Barents and Kara Seas. *Deep Sea Research Part I: Oceanographic Research Papers*, **49**(12),  
 1089 2281-2298 (doi: 10.1016/S0967-0637(02)00125-5)
- 1090 Sevestre H and Benn DI (2015) Climatic and geometric controls on the global distribution of surge-  
 1091 type glaciers: implications for a unifying model of surging. *Journal of Glaciology*, **61**(228),  
 1092 646-662 (doi: 10.3189/2015JoG14J136)
- 1093 Sharov AI and Tyukavina AY (2009) November. Mapping and interpreting glacier changes in  
 1094 Severnaya Zemlya with the aid of differential interferometry and altimetry. *Proceedings of*  
 1095 *Fringe 2009 Workshop, Frascati, Italy, 30 November-4 December 2009*, ESA Publication SP-  
 1096 677
- 1097 Sharov AI, Nikolskiy D, Troshko K and Zaprudnova Z (2015) Interferometric control for mapping and  
 1098 quantifying the 2012 breakup of Matusевич Ice Shelf, Severnaya Zemlya. *Proceedings of*  
 1099 *Fringe 2015 workshop, 23-27 March 2015, Frascati, Italy*, ESA Publication SP-731
- 1100 Sharp MJ (1985) Sedimentation and stratigraphy at Eyjabakkajökull: an Icelandic surging glacier.  
 1101 *Quaternary Research*, **24**, 268-284 (doi: 10.1016/0033-5894(85)90050-X)
- 1102 Sharp MJ (1988) Surging glaciers: geomorphic effects. *Progress in Physical Geography*, **12**, 533-559  
 1103 (doi: 10.1177/03091333880120040)
- 1104 Sommer C, Seehaus T, Glazovsky A and Braun MH (2022) Brief communication: Increased glacier  
 1105 mass loss in the Russian High Arctic (2010–2017). *The Cryosphere*, **16**(1), 35-42 (doi:  
 1106 10.5194/tc-16-35-2022)
- 1107 Stokes CR, Andreassen LM, Champion MR and Corner GD (2018) Widespread and accelerating glacier  
 1108 retreat on the Lyngen Peninsula, northern Norway, since their 'Little Ice Age'  
 1109 maximum. *Journal of Glaciology*, **64**(243), 100-118 (doi: 10.1017/jog.2018.3)
- 1110 Straneo F and Heimbach P (2013) North Atlantic warming and the retreat of Greenland's outlet  
 1111 glaciers. *Nature*, **504**(7478), 36-43 (doi: 10.1038/nature12854)
- 1112 Strozzi T, Paul F, Wiesmann A, Schellenberger T and Käab A (2017) Circum-Arctic changes in the flow  
 1113 of glaciers and ice caps from satellite SAR data between the 1990s and 2017. *Remote*  
 1114 *Sensing*, **9**(9) (doi: 10.3390/rs9090947)
- 1115 Svendsen JI and 10 others (1999) Maximum extent of the Eurasian ice sheets in the Barents and Kara  
 1116 Sea region during the Weichselian. *Boreas*, **28**(1), 234-242 (doi: 10.1111/j.1502-  
 1117 3885.1999.tb00217.x)

- 1118 Svendsen JI, Gataullin V, Mangerud J, Polyak L (2004) The glacial history of the Barents and Kara Sea  
 1119 region. In: Ehlers, J., Gibbard, P. (Eds.), Quaternary Glaciations—Extent and Chronology. Vol.  
 1120 1. Europe. Elsevier, Amsterdam.
- 1121 Tepes P, Gourmelen N, Nienow P, Tsamados M, Shepherd A and Weissgerber F (2021a.) Changes in  
 1122 elevation and mass of Arctic glaciers and ice caps, 2010–2017. *Remote Sensing of*  
 1123 *Environment*, **261** (doi: 10.1016/j.rse.2021.112481)
- 1124 Tepes P, Nienow P and Gourmelen N (2021b) Accelerating ice mass loss across Arctic Russia in  
 1125 response to atmospheric warming, sea ice decline, and Atlantification of the Eurasian Arctic  
 1126 Shelf Seas. *Journal of Geophysical Research: Earth Surface*, **126**(7) (doi:  
 1127 10.1029/2021JF006068)
- 1128 The IMBIE Team (2020) Mass balance of the Greenland Ice Sheet from 1992 to 2018. *Nature*, **579**,  
 1129 233-239 (doi: 10.1038/s41586-019-1855-2)
- 1130 Timokhov LA (1994) Regional characteristics of the Laptev and the East Siberian seas: climate,  
 1131 topography, ice phases, thermohaline regime, circulation. *Berichte zur Polarforschung*, **144**,  
 1132 15-31.
- 1133 van Pelt WJ and 6 others (2016) Multidecadal climate and seasonal snow conditions in  
 1134 Svalbard. *Journal of Geophysical Research: Earth Surface*, **121**(11), 2100-2117 (doi:  
 1135 10.1002/2016JF003999)
- 1136 Van Wychen, W and 6 others (2016) Characterizing interannual variability of glacier dynamics and  
 1137 dynamic discharge (1999–2015) for the ice masses of Ellesmere and Axel Heiberg Islands,  
 1138 Nunavut, Canada. *Journal of Geophysical Research: Earth Surface* **121**(1), 39–63. doi:  
 1139 10.1002/2015JF003708
- 1140 Williams M and Dowdeswell JA (2001) Historical fluctuations of the Matushevich ice shelf, Severnaya  
 1141 Zemlya, Russian high Arctic. *Arctic, Antarctic, and Alpine Research*, **33**(2), 211-222 (doi:  
 1142 10.1080/15230430.2001.12003424)
- 1143 Willis MJ, Melkonian AK and Pritchard ME (2015) Outlet glacier response to the 2012 collapse of the  
 1144 Matushevich Ice Shelf, Severnaya Zemlya, Russian Arctic. *Journal of Geophysical Research:*  
 1145 *Earth Surface*, **120**(10), 2040-2055 (doi: 10.1002/2015JF003544)
- 1146 Willis MJ and 10 others (2018) Massive destabilization of an Arctic ice cap. *Earth and Planetary*  
 1147 *Science Letters*, **502**, 146-155 (doi: 10.1016/j.epsl.2018.08.049)
- 1148 Zemp M and 10 others (2019) Global glacier mass changes and their contributions to sea-level rise  
 1149 from 1961 to 2016. *Nature*, **568**(7752), 382-386 (doi: 10.1038/s41586-019-1071-0)
- 1150 Zhao M, Ramage J, Semmens K and Obleitner F (2014) Recent ice cap snowmelt in Russian High  
 1151 Arctic and anti-correlation with late summer sea ice extent. *Environmental Research*  
 1152 *Letters*, **9**(4) (doi: 10.1088/1748-9326/9/4/045009)
- 1153 Zheng W and 6 others (2018) Accelerating glacier mass loss on Franz Josef Land, Russian  
 1154 Arctic. *Remote Sensing of Environment*, **211**, 357-375 (doi: 10.1016/j.rse.2018.04.004)
- 1155 Zheng W, Pritchard ME, Willis MJ and Stearns LA (2019) The possible transition from glacial surge to  
 1156 ice stream on Vavilov ice cap. *Geophysical Research Letters*, **46**(23), 13892-13902 (doi:  
 1157 10.1029/2019GL084948)

